Random-Key Algorithms for Optimizing Integrated Operating Room Scheduling

Bruno Salezze Vieira^{a,b,*}, Eduardo Machado Silva^{a,b}, Antônio Augusto Chaves^a

^a Federal University of São Paulo (UNIFESP), São José dos Campos, Brazil ^b Aeronautics Institute of Technology (ITA), São José dos Campos, Brazil

Abstract

Efficient surgery room scheduling is essential for hospital efficiency, patient satisfaction, and resource utilization. This study addresses this challenge by introducing a novel concept of Random-Key Optimizer (RKO), rigorously tested on literature and new, real-world inspired instances. Our combinatorial optimization problem incorporates multi-room scheduling, equipment scheduling, and complex availability constraints for rooms, patients, and surgeons, facilitating rescheduling and enhancing operational flexibility. The RKO approach represents solutions as points in a continuous space, which are then mapped in the problem solution space via a deterministic function known as a decoder. The core idea is to operate metaheuristics and heuristics in the randomkey space, unaware of the original solution space. We design the Biased Random-Key Genetic Algorithm with Q-Learning, Simulated Annealing, and Iterated Local Search for use within an RKO framework, employing a single decoder function. The proposed metaheuristics are complemented by lower-bound formulations, providing optimal gaps for evaluating the effectiveness of the heuristic results. Our results demonstrate significant lower and upper bounds improvements for the literature instances, notably proving one optimal result. Furthermore, the best-proposed metaheuristic efficiently generates schedules for the newly introduced instances, even in highly constrained scenarios. This research offers valuable insights and practical solutions for improving surgery scheduling processes, offering tangible benefits to hospitals by optimising resource allocation, reducing patient wait times, and enhancing overall operational efficiency.

Keywords: Surgery scheduling, Metaheuristic, Reinforcement learning, Random-key optimiser.

1. Introduction

Surgeries play a substantial role in hospital management. Their effective utilisation reduces surgical service delivery costs, shortens surgical patient wait times, and increases patient admissions (Roshanaei et al., 2017). To optimally manage the most relevant decisions and constraints related to it, the integrated surgery scheduling problem arises. It is a complex optimization problem that involves determining the optimal schedule for a set of surgical procedures, considering various constraints and objectives.

Multiple operating rooms (ORs) are available in a hospital for surgeries. The goal of integrated surgery scheduling is to allocate the available resting beds, ORs, Intensive Care Units (ICUs),

^{*}Corresponding author

Email addresses: bsvieira@unifesp.br (Bruno Salezze Vieira), machado.silva@unesp.br (Eduardo Machado Silva), antonio.chaves@unifesp.br (Antônio Augusto Chaves)

and Post-Surgery Care Units (PSCUs) to schedule surgical procedures in a way that maximizes room efficiency, reduces patient waiting times, and ensures the best utilization of resources.

From the patient's perspective, Figure 1 visually represents the surgery process. It begins with the patient arriving at the hospital and progressing through the following steps: (i) Resting room: Upon arrival, the patient is admitted and taken to a resting bed in the assessment area. Diagnostic tests and observation are conducted to assess the patient's medical condition; (ii) Operating Room (OR): Subsequently, the patient is taken to the OR to undergo the surgical procedure; (iii) Post-Surgery Care Unit (PSCU): After surgery, the patient is transferred to the PSCU for critical observation and anaesthesia recovery. This step ensures the patient's safe transition from the surgical procedure; (iv) Intensive Care Unit (ICU) (if applicable): Depending on the surgery's risk level or the patient's condition, there might be a scheduled transfer to the ICU for specialized care and monitoring; (v) Recovery Room: Following the critical observation and ICU (if required), the patient is taken back to the same room from step (i) for a recovery period. During this phase, the patient receives focused care and support to aid their healing process. Once the medical team determines the patient is stable and ready to leave the hospital, they are discharged (vi) with relevant post-surgery instructions and prescriptions, if necessary.

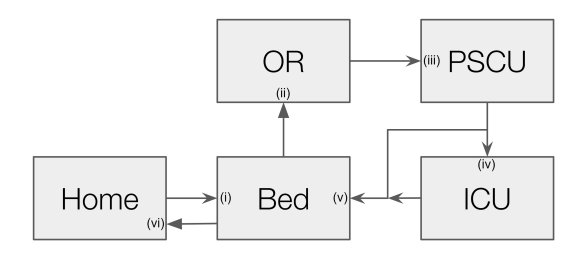


Figure 1: Patient surgery flow.

Considering this process, the problem we refer to as the Integrated Operating Room Scheduling Problem (IORSP) involves managing a set of surgical procedures, surgeons, operating rooms, and necessary equipment. A solution is to assign each patient to a suitable operating room based on predefined time slots at different stages within the previously outlined workflow. This allocation aims to schedule pending surgeries to minimize the total execution time, a metric referred to as makespan. This optimization problem takes into account a range of critical factors and constraints, which include:

- Surgeon availability: The scheduling process must account for the availability and preferences of surgeons. Surgeons often have different specialities and expertise, and their schedules must be synchronized with the allocated ORs. In this case study, each surgery already has a surgeon selected for it;
- Operating room allocation: The problem entails allocating surgical procedures to the available operating rooms (ORs), which are only accessible during business hours, to minimize idle time and maximize utilization. Additionally, certain surgeries may necessitate specific equipment or specialized facilities unique to certain ORs, which adds complexity to the allocation process;
- Surgery duration: Each surgical procedure has an estimated duration, which must be considered when scheduling surgeries sequentially. Accurate estimation of surgery duration is crucial for avoiding delays and conflicts. The patient's time in all surgery steps must be accounted for when scheduling the multiple rooms;
- Equipment availability: The availability of necessary equipment for different kinds of surgeries, such as ophthalmic and brain microscopes or video/endoscopy racks, is considered

during the scheduling process. Ensuring that all required resources are available at the right time is essential for smooth operations;

• Time constraints: The scheduling problem also consider time constraints, such as surgeon availability, business hours, moving time between rooms, and room maintenance post-use.

In our literature review, building upon the research of Xiang et al. (2015), Burdett and Kozan (2018), and Vali et al. (2022), we establish that the Integrated Operating Room Scheduling Problem (IORSP) can be effectively conceptualized and addressed as a variant of the Flexible Job Shop Problem (FJSP) (Brucker and Schlie, 1990). This research has been guided by the collaboration with a non-profit hospital that has unities in several cities in Brazil, basing our approach on a real-world case. This paper reviews existing literature alongside a comparative analysis with analogous scenarios and methodologies.

In this paper, we propose three metaheuristics using the Random-Key Optimizer (RKO) concept (Chaves et al., 2024) to solve the IORSP: Biased Random Key Genetic Algorithm with Q-Learning (BRKGA-QL) (Chaves and Lorena, 2021), Simulated Annealing (SA) (Kirkpatrick et al., 1983), and Iterated Local Search (ILS) (Lourenço et al., 2003). The BRKGA-QL has demonstrated efficacy without necessitating parameter fine-tuning, which is crucial for real-case hospital applications. Furthermore, we introduce two mathematical models for relaxed cases, enabling more efficient computation of lower bounds compared to a complete formulation (Chaudhry and Khan, 2016). Additionally, we tested available literature instances, adapting our methods to solve them successfully and comparing our results with existing literature methods. Finally, we designed, tested, and made a set of 20 instances based on our case study available online.

We can highlight our scientific contributions as:

- Proposal of two lower bound formulations that have small implementation complexity and yield better lower bounds than previous literature approaches;
- Investigation of flexible time constraints for each restricted schedule, where each room/surgeon's working hours can be delimited as available or not by the minute (one minute was our time discretization approach, but the user can change it);
- Introduction of a novel concept of a random-key optimizer with three metaheuristics using the same decoder process;
- Development of a parameter-less metaheuristic that performs better than tuned ones and literature algorithms for similar hospital cases.
- Validation of our methods against a similar literature case and demonstration of better results than previous ones;
- Complete modelling of a real-case scenario by procedurally generating 20 instances and making them available in a public repository;
- Demonstration of possible rescheduling using the same input data approach;

The remainder of the paper is structured as follows. In Section 2, we provide a literature review of the most similar works. In Section 3, we define the problem description. Section 4 details our proposed metaheuristics using the random-key concept, decoder, and reinforcement learning component. In Section 5, we present our experimental data, results, and analyses. In Section 6, we further discuss the results and conclude the paper. Our mathematical formulations to compute lower bounds are shown in Appendix A and Appendix B.

2. Literature review

The modeling of surgery scheduling problems commenced relatively early in deterministic models literature, among the first works we have Ozkarahan (1995). The authors developed software with multiple allocation models to schedule nurses, surgeon blocks, and surgeries and, followed by Dexter et al. (1999), studied bin packing algorithms and fuzzy constraints in operating room management and other works that followed.

Reviewing the literature, given how diverse hospital management is worldwide, the cases modelled after real-world cases rarely match each other, but they have enough similarities as we list them. Most works model the problem only scheduling the operating rooms (Abdelrasol et al., 2014). Among the works most similar to our approach, we have first the works of Fei et al. (2009), Fei et al. (2010), and Liu et al. (2011) that modelled OR allocation with five days of planning considering working hours and surgeon scheduling and solved using column generation and dynamic programming heuristics for procedurally generated instances and a Belgian university hospital case study. Molina-Pariente et al. (2015) proposed a case that may allocate an assistant surgeon to shorter surgery times. They proposed and implemented a constructive heuristic to solve it.

Aringhieri et al. (2015) modelled a case from the San Martino University Hospital, addressing simultaneous OR and recovery bed scheduling for a one-week planning horizon. Their model considers weekend stays without operations and various surgery specialities and is solved using a two-stage metaheuristic (assign and then schedule). Landa et al. (2016) extended the same case study into a stochastic variant, aiming to maximize OR utilisation and minimize overtime costs, and solved it using a hybrid simulation-based algorithm.

Xiang et al. (2015) treated the problem as an FJSP variant, scheduling pre and post-surgery rooms, nurses, and anaesthetists individually, similarly to our approach. They solved it with an Ant Colony metaheuristic. Marques and Captivo (2015) modelled a case of Lisbon's public hospital, allocating only ORs in a one-week planning horizon. The bi-objective problem maximizes the number of surgeries and room occupations with surgeon specialities and is solved with a bi-objective evolutionary metaheuristic.

Durán et al. (2017) modelled a case of a Chilean public hospital and developed two models for scheduling interventions on top of an existing OR schedule over a defined period that satisfies patient priority criteria. Dellaert and Jeunet (2017) modelled a case of a Dutch cardiothoracic centre for a 4-week planning horizon, considering the allocation of beds, ORs, and ICUs and maximizing the number of scheduled surgeries. The authors proposed a mathematical model and a Variable Neighbourhood Search (VNS) metaheuristic that found better results than the model solved with CPLEX in all cases. Siqueira et al. (2018b) solved a stochastic model for a long-term plan from a case study of the Brazilian National Institute of Traumatology and Orthopedics, which considers OR and recovery ward allocations with downstream constraints, using simulations and optimal action-taking.

Burdett and Kozan (2018) modelled a case of a university and college-affiliated teaching hospital in Brisbane, Australia, as an FJSP considering bed, OR, PSCU, and ICU allocation. They presented and made available 24 generated instances, and to solve it, they proposed some initial solution heuristics and a Hybrid Simulated Annealing (HSA) as its main algorithm. Hamid et al. (2019) modelled a public hospital case in Tehran as a multi-objective problem. They schedule ORs considering patient priorities and surgical team members' decision-making styles to improve the surgical teams' compatibility level, minimizing the total cost, overtime OR utilisation, and maximizing team consistency. They presented a mathematical model and implemented two metaheuristics to obtain better solutions: a Non-dominated Sorting Genetic Algorithm (NSGA-II) and a Multi-Objective Particle Swarm Optimisation (MOPSO).

Roshanaei et al. (2020) proposed Branch-and-check methods for operating room planning and scheduling with surgeon specialities for patient surgeon assignment and priorities. Their exact methods outperformed conventional integer formulation approaches by a large margin using the benchmark instances of Marques and Captivo (2015) and a procedurally generated one. Zhu et al. (2020) solved a case study of an affiliated hospital of the University of Science and Technology of China, maximizing OR utilisation on a one-week planning horizon, OR to surgery to surgeon assignment, and patient priorities. The authors presented a mathematical formulation and two hybrid metaheuristics to obtain better solutions. Thomas Schneider et al. (2020) studied the surgery groups scheduling considering ORs and downstream beds operating with different available hours with a 15-day planning horizon, modelled of the Leiden University Medical Center, proposed a single step integer model that maximizes OR usage and minimises bed usage variation with weights, they also tested the van Essen et al. (2014) instances lowering the amounts of required beds upon the previous results.

More recently, Lin and Li (2021) solved a case of surgery to OR assignment, five days planning horizon and minimizing the operation costs and overtime usage, provided an improved mathematical model of Fei et al. (2009) and a metaheuristic Artificial Bee Colony (ABC) that obtained better solutions for larger instances. Park et al. (2021) modelled a case of a Korean university hospital considering surgeons' preferences and cooperative operations, in which surgery can have multiple surgeons cooperatively sequentially to reduce its execution time, and the co-oped surgeries have a lower total execution time. This feature helps to minimize the total overtime and the number of ORs used. A mathematical model and a metaheuristic were proposed to solve it.

Table 1 comprises the similarities found during our literature review for the modelled real-world case studies, the case study they were based on, if it was solved with an exact (E) or heuristic (H) method, objective function focus, and the problem attributes: surgery to surgeon assignment (SSA), multi-room scheduling (MRS), time slots allocation (TS), patient priorities (PP), surgeon specialities (SE), a limited planning horizon (PH), overtime costs (OT), and other resources scheduling (ORS) like nurses, anaesthetists or equipment.

Table 1: Case study comparisons with similar literature works.

Paper	Case study	E	Η	Objective Function	SSA	MRS	TS	PP	$_{ m SE}$	$_{\mathrm{PH}}$	OT	ORS
Fei et al. (2009, 2010); Liu et al. (2011)	Belgian university hospital	X	X	Costs			X			X	X	
Aringhieri et al. (2015); Landa et al. (2016)	San Martino university hospital	X	X	Costs			X		X	X		
Marques and Captivo (2015)	Public hospital in Lisbon		X	Usage			X	X	X	X		
Xiang et al. (2015)	-		X	Makespan	X	X	X		X		X	X
Durán et al. (2017)	Public hospital in Chile		X	Usage	X			X	X	X	X	
Dellaert and Jeunet (2017)	Dutch cardiothoracic center	X	X	Usage		X				X		
Burdett and Kozan (2018)	Hospital in Brisbane, Qld, Australia		X	Makespan		X	X					
Hamid et al. (2019)	Public hospital in Tehran	X	X	Usage and MSWT			X	X		X	X	
Roshanaei et al. (2020)	Public hospital in Lisbon	X		Usage	X		X		X	X		
Zhu et al. (2020)	Affiliated one of UST of China		X	Costs	X				X	X	X	
Thomas Schneider et al. (2020)	Leiden University Medical Center	X	X	Usage			X		X	X	X	
Yazdi et al. (2020)	Medium-sized Norwegian Hospital	X		#Surgeries	X	X	X			X		
Akbarzadeh et al. (2020)	Sina Hospital (Tehran, Iran)	X	X	Costs			X			X		X
Park et al. (2021)	Korean university hospital	X	X	Active ORs and OT			X				X	X
This Work	Non profit hospital in Brazil	X	X	Makespan		X	X	X				X

For more comprehensive reviews of ORSP models, including models with uncertainty, stochastic, and mixed approaches, we advise the works of Abdelrasol et al. (2014). Van Riet and Demeulemeester (2015) presented a review focused on the trade-offs in operating room planning for electives and emergencies, and Rahimi and Gandomi (2021) accomplished analysis and classified solution approaches similarly to Abdelrasol et al. (2014), with deterministic and probabilistic approaches, performance metrics and its trends throughout time.

3. Problem definition

Given the literature review and problem characteristics, we model the IORSP as an FJSP variant. The FJSP is usually described as having a set of jobs K to be processed by the machines of set R, each job consists of a sequenced set T_k of tasks, and each task t has to be performed sequentially to complete the job. For each job k, $k \in K$, the execution of task t, $t \in T_k$, requires one machine r out of a set of given machines R_t , $R_t \subset R$, that execute task t. For task t running on machine r, $r \in R_t$, the task time is γ_t^d , the setup time is γ_t^m and cool-down time is γ_t^c . When a task t is complete, but the allocated machine $r \in R_{Next(t)}$ is not immediately available, the start of task Next(t) is delayed. This delay is called blocking, with a blocking limit per task ϕ_t .

Moreover, the FJSP typically follows some assumptions as we do, as the machines and jobs are always available. Once started, an operation cannot be interrupted. There is no precedence among the tasks of different jobs; each task can be processed by only one machine at a time. As the objective function, FJSP usually minimizes the makespan, that is, the amount of time required to complete all jobs or to maximize the total of completed jobs given a planning horizon.

We can translate the FJSP nomenclature to our problem, considering jobs as surgeries and machines as subjects (rooms, types of equipment, and surgeons). Each surgery consists of a sequence of tasks. Our problem has some particularities, like a non-empty initial schedule or simultaneous machines for the same task, as operations (tasks) require a surgeon, which may require some equipment and OR, i.e., different types of machines (subjects) allocated simultaneously. All γ_t^d , γ_t^m and γ_t^c are fixed for any particular subject, so they are called duration (γ_t^d) , moving time (γ_t^m) and cleaning time (γ_t^c) . The name blocking is a homonym in our work, and we have a fixed blocking limit Φ for all tasks of 15 minutes. Each subject (machine) has its initial availability schedule (structure we call availability slots). As an FJSP variant, the surgery is a job that requires heterogeneous machines working on the same task during the same period to complete it. In our approach, we only tackled minimizing the makespan. We note that maximizing the number of surgeries tends to prioritize the shorter surgeries.

Table 2 shows our modelled structures for our mathematical notations. We can divide them between static and dynamic structures. Among our static structures, the input data consists of a set of equipment E_f for each equipment type f, sets R^{bed} and R^{or} representing the beds and operation rooms, respectively, a set of surgeries K, and each surgery k to be scheduled has a set of tasks T_k . Each task k has a set of required people L_t (in our case study, this set primarily includes patients for all tasks and the assigned surgeon for each surgery), set of required equipment types F_t , set of compatible rooms R_t , expected duration time γ_t^d , moving time γ_t^m and cleaning time γ_t^c . There is an initial set of availability slots for each one of our resources (person, equipment, or room).

Figure 2 illustrates the concept of availability slots (AS), a timeline for any subject with available and unavailable intervals. The numbers and arrows on the illustration point to the corresponding hour an interval starts or ends. In this example $W = \{0, 15, 24, 39, 72, 87, 120\}$, the subject is available for the first 15 hours, becomes unavailable for 9 hours (15 to 24), is available again for 15 hours (24 to 39), becomes unavailable for the next 33 hours (39 to 72), and so on. This AS example could be the availability of a surgeon, operating room, or other subjects. Mathematically, we define W as an ordered set of time instants arranged in increasing order. The initial element signifies the first available time instant, while the subsequent elements represent an alternation of unavailable and available time instants. This data structure is used as an initial timeline availability and is dynamically adjusted per solution.

Furthermore, our modelling allows tackling the re-scheduling of surgeries. Surgery re-scheduling is crucial for effectively managing the IORSP due to the hospital environment's dynamic and

Table	e 2: Problem data notations	
\mathbf{Sets}		
E_f	Equipment of type f	
$\mathring{R^{or}}$	All OR rooms	
R_{bed}	All bed rooms	
K	Surgeries	
T_k	Tasks of surgery k	
L_t	People allocated for task t	
F_t	Equipment types required for task t	
R_t	Compatible rooms for task t	
Attributes		
γ_t^d	Duration time of task t	
γ_t^m	Moving time of task t	
γ^c_t	Cleaning time of task t	
0 15 24 39	72 87	120
† † † †	.	V
24h 24h	24h 24h 24h	

Figure 2: Example of a set of availability slots (AS) for a subject.

unpredictable nature. It allows for flexibility and adaptability in emergencies, resource availability fluctuations, and changes in patient conditions. Re-scheduling ensures that urgent surgeries can be accommodated without significant disruptions, minimizes delays and wait times, and optimizes the use of resources. Additionally, it helps cope with cancellations and no-shows by filling gaps efficiently, maintaining high productivity levels, and ensuring timely surgical care. To implement surgery re-scheduling efficiently, we make use of the sets of availability slots with the previously fixed schedules for rooms, patients, equipment and surgeons as shown in detail in Section 5.3.

Appendix A and Appendix B preset the relaxed models we propose and implement to compute lower bounds to minimize each instance's makespan. The resulting lower bounds are used to analyze the performance of the heuristics, and smaller gaps imply a strong performance of both proposals. Both models solve a relaxed case of the IORSP and exploit the fact that, for the case study and the literature case, the bed is reserved during the entire patient's stay in the hospital. It considers a best-case scenario execution for all surgeries and only allocates surgeries to rooms but does not sequence any task. All patients are treated without delays (blocking), disregarding room or surgeon-restricted schedules, sequencing of tasks, and equipment availability. Removing these constraints, the relaxed problem solved by both models is an allocation problem.

4. Random-Key Optimizer

The random-key representation was first proposed by Bean (1994) for an extension of the genetic algorithm called the Random-key Genetic Algorithm (RKGA). This representation encodes a solution with random numbers in the interval [0,1). The main idea is that the RKGA searches the random-key space as a surrogate for the original solution space. Points in the random-key space are mapped to points in the original solution space by a deterministic algorithm called the decoder. An advantage of this encoding is its robustness to problem structure, as it separates the solver (solution procedure) from the problem being solved. The connection between the solver and the problem is established through the decoder.

A Random-key Optimizer (RKO) is an optimization heuristic that solves specific problems by exploring the continuous random-key space $[0,1)^n$, where n is the size of the random-key vector that encodes the problem solution. The pioneer of this approach is the work of Bean (1994), which utilizes a genetic algorithm to perform searches in the solution space for various optimization problems. In Gonçalves and Resende (2011), a variation of the RKGA called Biased RKGA (BRKGA) is proposed and evaluated for a wide range of optimization problems. Later, the RKO framework was employed by Schuetz et al. (2022) for robot motion planning, using the BRKGA and an extension of Simulated Annealing to search the random-key space. In Mangussi et al. (2023), the RKO is implemented using Simulated Annealing, Iterated Local Search, and Variable Neighbourhood Search for the tree hub location problem. Recently, Chaves et al. (2024) proposed an RKO considering the GRASP metaheuristic and evaluates it for the travelling salesman problem, tree hub location problem, Steiner triple covering problem, node capacitated graph partitioning problem, and job sequencing and tool switching problem. Figure 3 presents the RKO concept where \mathcal{D} represents the specific decoder algorithm.

The optimization process is shown in Figure 3(a). This process takes as input an instance of a combinatorial optimization problem and returns the best solution found, guided by a specified metaheuristic. Figure 3(b) illustrates the mapping schema that connects the random-key representation to the solution space through a problem-specific decoder. After this transformation, the quality of the solutions can be evaluated. Finally, Figure 3(c) presents an example of a decoder process for a scheduling-based problem. In this case, each vector position represents a task or characteristic of the optimization problem. The decoder works by sorting the random keys, where the sorted indices correspond to a potential solution obtained by arranging the tasks in the specific order dictated by the sorted keys.

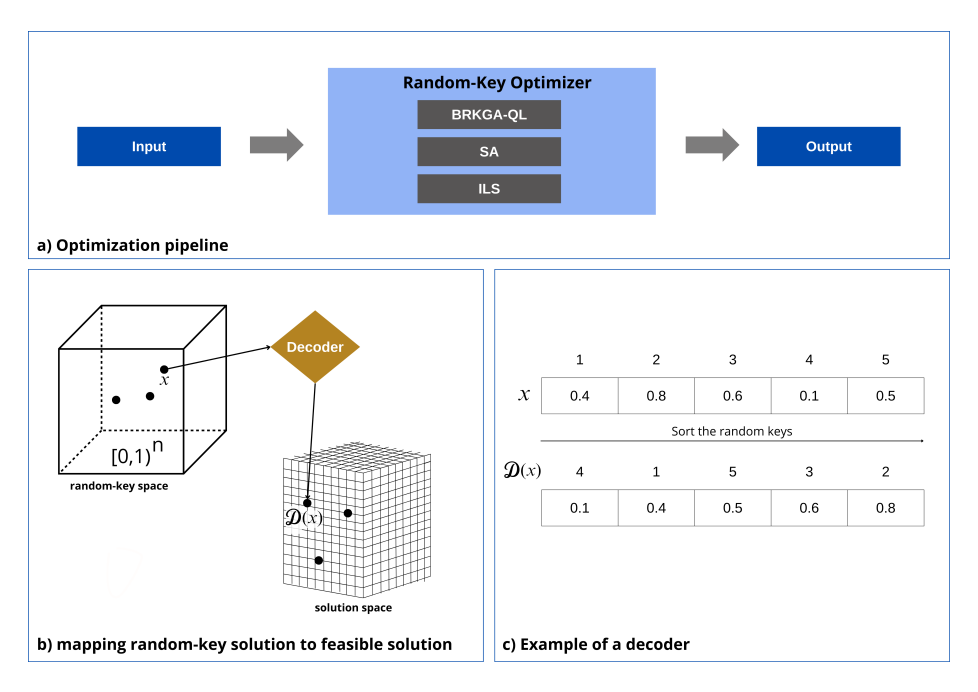


Figure 3: Random-Key Optimizer concept. Based on Schuetz et al. (2022).

In the remainder of this section, we introduce the RKO framework. We begin by discussing its key components (subsection 4.1), followed by an overview of the metaheuristics utilized in the framework. Specifically, we present the BRKGA-QL (subsection 4.2), Simulated Annealing (subsection 4.3), and Iterated Local Search algorithms (subsection 4.4), which operate on the random-key vectors within the proposed RKO framework.

4.1. RKO Components

The RKO components are procedures embedded within the framework's random-key space that support the search process's metaheuristics balance between diversification and intensification. These components include shaking, blending, and local search performed by the Random Variable Neighbourhood Descent (RVND) method on the random-key vectors. Each of these components is described in detail below.

4.1.1. Shaking

The shaking method was inspired by the approach proposed by Andrade et al. (2019). The method modifies random-key values by applying random modifications considering four distinct neighbourhood moves. A perturbation rate β is employed. This value is randomly generated within a specified interval $[\beta_{min}, \beta_{max}]$, which should be defined according to the specific metaheuristic approach being used. The four movements are:

- Swap: Swap the positions of two randomly selected random keys i and j.
- Swap Neighbor: Swap the position of a randomly selected random key i with its neighboring key i + 1.
- Mirror: Change the value of a randomly selected random key i with its complementary value
- Random: Assigns a new random value within the interval [0,1) to a randomly selected random key i.

Algorithm 1 described the shaking procedure. First, a shaking rate β is randomly generated within the interval $[\beta_{min}, \beta_{max}]$, determining the number of perturbations to be applied, specifically $\beta \times n$, where n is the length of the random-key vector A. For each perturbation, a random shaking move is selected from four options: a random move, a mirror move, a swap move, or a swap neighbor move. The selected move is then applied to the vector A. After all perturbations are performed, the modified vector is returned as the output. This vector is then decoded during the metaheuristics search process.

4.1.2. Blending

The blending method extends the uniform crossover (UX) concept proposed by Davis (1991) by introducing stochastic elements to create a new random-key vector. The algorithm combines two solutions, A^a and A^b , to generate a new solution A^c . For each position i in the vector, a random decision is made based on a probability ρ to inherit the corresponding key from either A^a or A^b . The algorithm introduces a parameter factor, which modulates the contribution of A^b . Specifically, when factor = 1, the original key from A^b is used, and when factor = -1, the complement $(1.0 - A_i^b)$ is considered. Additionally, with a small probability μ , the algorithm generates a new random value within the interval [0, 1), further diversifying the resulting vector A^c . The algorithm's pseudocode is presented in Algorithm 2.

4.1.3. Random Variable Neighbourhood Descent

The Variable Neighbourhood Descent (VND) was proposed by Mladenović and Hansen (1997) and extended later for various optimization problems. The VND consists of a finite set of preselected neighbourhood structures denoted by N_k for $k = 1, ..., k_{max}$, where $N_k(A)$ represents the set of solutions in the k-th neighborhood of a random-key vector A. While standard local

Algorithm 1: Shaking method

```
Input: Random-key vector A, \beta_{min}, \beta_{max}
   Output: Changed random-key vector A
 1 Generate shaking rate \beta randomly within the interval [\beta_{min}, \beta_{max}];
 2 for k \leftarrow 1 to \beta \times n do
       Randomly select one shaking move m from \{1, 2, 3, 4\};
 3
       switch m do
 4
          case 1 do
 5
              Apply Random move in A;
 6
          end
 7
          case 2 do
 8
           Apply Invert move in A;
 9
          end
10
          case 3 do
11
12
              Apply Swap move in A;
          end
13
          case 4 do
14
             Apply Swap Neighbor move in A;
15
          end
16
       end
17
18 end
19 return A;
```

Algorithm 2: Blending method

```
Input: Random-key vector A^a, Random-key vector A^b, factor, \rho, \mu
   Output: New random-key vector A^c
 1 for i \leftarrow 1 to n do
       if UnifRand(0,1) < \mu then
            A_i^c \leftarrow \text{UnifRand}(0,1);
 3
       end
 4
       else
 5
            if UnifRand(0,1) < \rho then
 6
               A_i^c \leftarrow A_i^a
 7
 8
            end
 9
            else
                if factor = 1 then
10
                 A_i^c \leftarrow A_i^b
11
                end
12
                if factor = -1 then
13
                    A_i^c \leftarrow 1.0 - A_i^b
14
                \quad \text{end} \quad
15
            end
16
17
       end
18 end
19 return A^c;
```

search heuristics typically employ a single neighborhood structure, VND utilizes multiple structures to enhance the search process. Key considerations for applying VND include determining which neighborhood structures to use and their sequence and selecting an appropriate search strategy for switching between neighborhoods. Later, Penna et al. (2013) proposed the RVND. RVND randomly selects the neighborhood heuristic order to be applied in each iteration. RVND efficiently explores diverse solution spaces and can be applied to random-key spaces. Users can implement classic heuristics for the specific problem and encode the locally optimal solution into the random-key vector after the search process. Alternatively, users can implement random-key neighborhoods independent of the specific problem, using the decoder to converge towards better solutions iteratively.

Algorithm 3 displays the RVND pseudo-code. Given an initial solution A, the algorithm begins by initializing a Neighborhood List (NL). While the NL is not empty, a neighborhood \mathcal{N}^i is selected randomly from it, and the best neighbor A' within \mathcal{N}^i is identified. If the objective function value $\delta_{\mathcal{D}(A')}$ improves upon the current solution $\delta_{\mathcal{D}(A)}$, the current solution A is updated to A', and the NL is reset. If no improvement is found, the selected neighborhood \mathcal{N}^i is removed from the NL. The process repeats until all neighborhoods have been explored without finding a better solution. The algorithm then returns the best solution found.

```
Algorithm 3: RandomVND
    Input: A
    Output: The best solution in the neighbourhoods.
 1 Initialise the Neighbourhood List (NL);
   while NL \neq 0 do
        Choose a neighbourhood \mathcal{N}^i \in NL at random;
 3
        Find the best neighbour A' of A \in \mathcal{N}^i;
 4
        if \delta_{\mathcal{D}(A')} < \delta_{\mathcal{D}(A)} then
 5
 6
            A \leftarrow A';
            Restart NL;
 7
        else
 8
            Remove \mathcal{N}^i from the NL;
 9
10 return A
```

Next, we introduce four problem-independent local search heuristics designed to operate within the random-key space. These heuristics employ distinct neighborhood structures for the RVND algorithm, specifically used to identify the best neighbors as described in line 4 of Algorithm 3. The neighborhood structures include Swap LS, Mirror LS, Farey LS, and Nelder-Mead LS.

4.1.4. Swap Local Search

The Swap local Search focuses on interchanging two values within the random-key vector. The local search procedure considering this structure is outlined in Algorithm 4. The algorithm begins by defining a vector RK with random order for the random-key indices and initialises the best solution found, A^{best} , to the current solution A. It then iterates over all pairs of indices i and j (with j > i) in the random-key vector. For each pair, it swaps the value of the random keys at indices RK_i and RK_j in A. If the resulting solution has a better objective function value than A^{best} , it updates A^{best} to the new solution. If not, it reverts A to the previous best solution. The process continues until all pairs have been considered. The algorithm returns A^{best} as the best random-key vector found in the neighborhood.

Algorithm 4: Swap Local Search

```
Input: Random-key vector A
   Output: Best random-key vector A^{best} found in the neighborhood
 1 Define a vector RK with random order for the random-key indices;
 2 Update the best solution found A^{best} \leftarrow A:
   for i \leftarrow 1 to n-1 do
       for j \leftarrow i + 1 to n do
            Swap random keys RK_i and RK_i of A;
 5
           if \delta_{\mathcal{D}(A)} < \delta_{\mathcal{D}(A^{best})} then
 6
             A^{best} \leftarrow A;
 7
            else
 8
            A \leftarrow A^{best};
10 return A^{best};
```

4.1.5. Mirror Local Search

The Mirror Local Search perturbs the random-key values, changing the current value in position j to (1 - A[j]). Algorithm 5 illustrates this procedure. Initially, it defines a vector RK with a random order for the random-key indices and sets the best solution found, A^{best} , to the current solution A. The algorithm then iterates over all indices i in the random-key vector A. For each index, it inverts the value of the random key at RK_i . After each inversion, if the new solution has a better objective function value than A^{best} , it updates A^{best} to the new solution. If not, it reverts A to A^{best} . This process continues until all indices have been processed. Finally, the algorithm returns A^{best} as the best random-key vector found in the neighborhood.

```
Algorithm 5: Mirror Local Search
  Input: Random-key vector A
  Output: Best random-key vector A^{best} found in the neighborhood
1 Define a vector RK with random order for the random-key indices;
2 Update the best solution found A^{best} \leftarrow A;
3 for i \leftarrow 1 to n do
      Change the value of the random key RK_i of A to its complement;
4
      if \delta_{\mathcal{D}(A)} < \delta_{\mathcal{D}(A^{best})} then
       A^{best} \leftarrow A;
7
       A \leftarrow A^{best};
9 return A^{best};
```

4.1.6. Farey Local Search

The Farey Local Search modifies the value of each random key by randomly selecting values between consecutive terms of the Farey sequence Niven et al. (1991). The Farey sequence of order η consists of all completely reduced fractions between 0 and 1, with denominators less than or equal to η , arranged in increasing order. For our purposes, we use the Farey sequence of order 7:

$$F_7 = \left\{ \frac{0}{1}, \frac{1}{7}, \frac{1}{6}, \frac{1}{5}, \frac{1}{4}, \frac{2}{7}, \frac{1}{3}, \frac{2}{5}, \frac{3}{7}, \frac{1}{2}, \frac{4}{7}, \frac{3}{5}, \frac{2}{3}, \frac{5}{7}, \frac{3}{4}, \frac{4}{5}, \frac{5}{6}, \frac{6}{7}, \frac{1}{1} \right\}$$

In each iteration of the heuristic, the random keys are processed in a random order. Algorithm 6 illustrates this procedure. It begins by defining a vector RK with a random order for the random-key indices and initialises the best solution found, A^{best} , to the current solution A. The algorithm then iterates over each index i in the random-key vector. For each index i, it iterates over the Farey sequence F of fractions, setting the value of the random key RK_i in A to a random value uniformly generated between F_j and F_{j+1} , where F_j and F_{j+1} are consecutive fractions in the Farey sequence. After updating the random key RK_i , if the new solution has a better objective function value than A^{best} , it updates A^{best} to the new solution. If not, it reverts A to A^{best} . The algorithm continues this process until all indices have been processed. Finally, the algorithm returns A^{best} as the best random-key vector found in the neighborhood.

```
Algorithm 6: Farey Local Search
```

```
Input: Random-key vector A
    Output: Best random-key vector A^{best} found in the neighborhood
 1 Define a vector RK with random order for the random-key indices;
 2 Update the best solution found A^{best} \leftarrow A;
   for i \leftarrow 1 to n do
        for j \leftarrow 1 to |F| do
 4
            Set the value of the random key RK_i of A with UnifRand(F_i, F_{i+1});
 5
            if \delta_{\mathcal{D}(A)} < \delta_{\mathcal{D}(A^{best})} then
 6
                A^{best} \leftarrow A;
 7
 8
             A \leftarrow A^{best};
10 return A^{best};
```

4.1.7. Nelder-Mead Local Search

The Nelder–Mead Local Search, introduced by Nelder and Mead (1965), is a numerical technique for finding the minimum of an objective function in a multidimensional space. This direct search approach relies on function comparisons and is commonly used in derivative-free nonlinear optimization. The method starts with at least three solutions and can perform five moves: reflection, expansion, inside contraction, outside contraction, and shrinking. In this study, we always apply the Nelder-Mead Local Search with three solutions: A_1 , A_2 , and A_3 , where one is the current solution derived from the metaheuristic, while the others are randomly chosen from a pool of elite solutions found during the search process. These solutions are ordered by objective function value (A_1 is the best and A_3 is the worst). Figure 4 illustrates a simplex polyhedron and the five moves.

Algorithm 7 presents the pseudo-code for the Nelder-Mead Local Search adapted for discrete optimization problems. We employ the blending method (Algorithm 2) to generate new solutions, using $\rho = 0.5$ and $\mu = 0.02$. The algorithm begins with an initial simplex of three solutions (A_1, A_2, A_3) . The simplex is sorted based on the objective function values, and the simplex's centroid (A_0) is computed between A_1 and A_2 (A_0) = Blending $(A_1, A_2, 1)$. The main loop iterates until a termination condition is met. The algorithm performs a series of moves on the simplex during each iteration to explore the search space. A reflection solution (A_r) = Blending $(A_0, A_3, -1)$ is computed. If the objective function value at A_r is better than the current best solution (A_1) , the algorithm computes an expansion solution (A_e) = Blending $(A_r, A_0, -1)$. If the objective function value at A_e is better than at A_r , A_0 is replaced by A_e ; otherwise, A_0 is replaced by A_r . If neither the reflection nor the expansion improves the solution, the algorithm contracts towards the solution A_r or A_0 . For an outside contraction (when A_r is better than A_0), the contraction

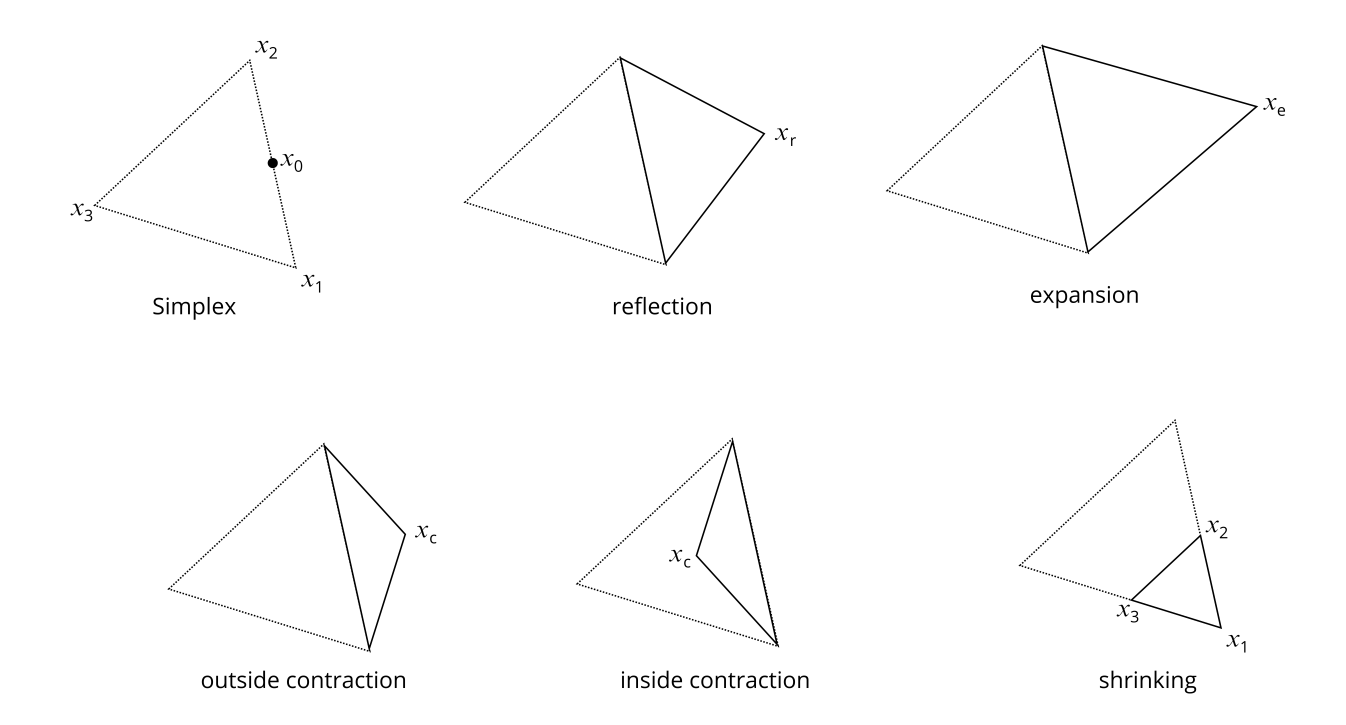


Figure 4: Illustrative example of the simplex polyhedron and the five moves of the Nelder-Mead Local Search. Source: Chaves et al. (2024).

solution is $A_c = \text{Blending}(A_r, A_0, 1)$. For an inside contraction (when A_r is not better than A_3), the contraction solution is $A_c = \text{Blending}(A_0, A_3, 1)$. If the contraction step does not improve, the entire simplex is shrunk towards the best solution A_1 ($A_i = \text{Blending}(A_1, A_i, 1), i = 2, 3$). The algorithm terminates when the maximum number of iterations equals $n \times e^{-2}$.

4.2. Biased Random-Key Genetic Algorithm with Q-Learning

The BRKGA was introduced by Gonçalves and Resende (2011) and modifies the RKGA by incorporating bias into the parent selection and crossover operators during the evolutionary process. Specifically, BRKGA starts its search process by initializing an initial population denoted as P, consisting of randomly generated |P| individuals. In each subsequent generation, these individuals are evaluated based on their fitness, being classified into two distinct groups. The elite population, denoted as $P_e \subset P$, contains the better individuals in terms of fitness. The other group includes non-elite individuals $(P - P_e)$.

An individual's fitness is predicated on the resultant value yielded by the objective function (Gonçalves and Resende, 2011). In the course of evolution, a new population emerges through a two-step procedure: first, by replicating the elite partition P_e from the current generation, and then, by introducing a novel group of mutants referred to as P_m . The quantity of mutants is proportional to the size of the population. The offspring set is denominated as P_c and is produced using the parameterized uniform crossover (PUX) operator (Spears and De Jong, 1991) to complete the new population.

The new population is thus comprised of three distinct parts: i) the elite partition P_e , ii) the

Algorithm 7: Nelder-Mead Local Search. Source: Chaves et al. (2024).

```
Data: A_1, A_2, A_3, n
    Result: The best solution found in simplex X
 1 begin
          Initialize simplex: X \leftarrow \{A_1, A_2, A_3\};
 2
          Sort simplex X by objective function value;
 3
          Compute the simplex centroid A_0 \leftarrow \text{Blending}(A_1, A_2, 1);
 4
          iter \leftarrow 0;
 5
         numIter \leftarrow n \cdot |1.0/h|;
 6
          while iter < numIter do
 7
               shrink \leftarrow 0;
 8
               iter \leftarrow iter + 1 \ ;
 9
               Compute reflection solution A_r \leftarrow \text{Blending}(A_0, A_3, -1);
10
               if \delta_{\mathscr{D}(A_r)} < \delta_{\mathscr{D}(A_1)} then
11
                     Compute expansion solution A_e \leftarrow \text{Blending}(A_r, A_0, -1);
12
                     if \delta_{\mathscr{D}(A_e)} < \delta_{\mathscr{D}(A_r)} then
13
                       \  \  \, \bigsqcup \ A_3 \leftarrow A_e \ ;
14
                     else
15
                       16
               else
17
                     if \delta_{\mathscr{D}(A_r)} < \delta_{\mathscr{D}(A_2)} then
18
                      \[ A_3 \leftarrow A_r ; \]
19
                     else
20
                           if \delta_{\mathscr{D}(A_r)} < \delta_{\mathscr{D}(A_3)} then
21
                                Compute contraction solution A_c \leftarrow \text{Blending}(A_r, A_0, 1);
22
                                if \delta_{\mathscr{D}(A_c)} < \delta_{\mathscr{D}(A_r)} then
23
                                  24
                                else
25
                                  | shrink \leftarrow 1 ;
26
                           else
27
                                Compute contraction solution A_c \leftarrow \text{Blending}(A_0, A_3, 1);
28
                                if \delta_{\mathscr{D}(A_c)} < \delta_{\mathscr{D}(A_3)} then
29
                                  A_3 \leftarrow A_c;
30
                                else
31
                                  | shrink \leftarrow 1 ;
32
               if shrink = 1 then
33
                 Replace all solutions except the best A_1 with A_i \leftarrow \text{Blending}(A_1, A_i, 1), i = 2, 3;
34
               Sort simplex X by objective function value;
35
               Compute the simplex centroid A_0 \leftarrow \text{Blending}(A_1, A_2, 1);
36
37
         return A_1;
```

mutant partition P_m , and iii) the offspring set P_c derived from PUX. This operator process hinges on a parameter ρ_e , which governs the likelihood of an offspring inheriting a gene (or vector component) from an elite parent instead of a non-elite parent. A random number is generated for each gene within an offspring. Should this random number be less than ρ_e , the corresponding gene is inherited from the elite parent's random key; otherwise, it is inherited from the non-elite parent's random key. After this, a decoding mechanism is applied to each individual, mapping the chromosome into a problem solution.

In the version of the BRKGA implemented in this paper, the new population comprises only two components: i) the elite partition P_e and ii) the offspring set P_c . The crossover operator is the blending procedure (see subsection 4.1.2) with factor = 1 rather than the PUX method. As a result, the role of mutants is replaced by introducing a mutation operator directly within the blending method (lines 2–3 of Algorithm 2).

The individuals are then evaluated and sorted based on their fitness. This evolutionary process continues until a predetermined stopping criterion, such as attaining a maximum number of generations, is fulfilled. Additional configurable parameters of the BRKGA encompass the population size (|P|), the proportion of individuals contained within the elite partition (p_e , where $|P_e| = |P| \times p_e$), and the probability of mutation (μ).

The BRKGA-QL (Chaves and Lorena, 2021) differs from the just presented BRKGA. The first aspect is the replacement of mutants by mutations. Before gene selection from either parent, a mutation may occur with a probability of μ . If positive, the gene acquires a random value within the range of [0,1); otherwise, the gene is inherited based on a probability ρ_e , with preference given to the elite parent, and if not, it is inherited from the non-elite parent. Secondly, using a Q-Learning agent, it dynamically adjusts the parameter values $(p, p_e, \mu, \text{ and } \rho_e)$. Finally, we have a local search module coupled at the end of each generation. A clustering method is applied to identify promising regions, and an intensification is performed to accelerate the convergence of the method. The RVND (see section 4.1.3) is used as the local search component. Detailed information about this Q-learning agent can be found in the following section.

4.2.1. Q-Learning

The parameter selection process represents an additional optimization challenge, typically addressed through a parameter tuning procedure for later static parameter executions. Such procedure often entails selecting parameter ranges manually or through automation in most existing works (Dang et al., 2017). In contrast, the Q-Learning process offers an automated parameter-tuning mechanism that runs parallel to the main problem-solving algorithm.

Considered one of the most relevant contributions to Reinforcement Learning, the Q-Learning algorithm (Watkins and Dayan, 1992) is a model-free algorithm (off-policy) that establishes the policy of actions interactively. This algorithm does not require complete modelling of the environment to determine which optimal policy to apply. It is capable of learning from the experiences obtained.

Q-Learning has its domain modelled as a Markov Decision Process (Sutton and Barto, 1999). It consists of the learning process of the agent inserted in an environment in terms of actions a, states s, and rewards r. Equation (1) shows the calculations for updating the weights of state-action pairs. Function Q delineates the value associated with the state-action pair (s,a) at the Q-table i+1, symbolising the quality of actions taken to anticipate future returns or rewards. This update is contingent on two parameters: the learning factor, denoted as λ^{lf} , and the diversification factor, denoted as λ^{df} .

$$Q^{i+1}(s,a) := Q^{i}(s,a) + \lambda^{lf}[R^{i}(s,a) + \lambda^{df} \times \max_{a'} Q^{i}(s',a') - Q^{i}(s,a)]$$
(1)

Moreover, analogous to metaheuristic common practices, the Q-Learning execution tends to take the best-known actions for each state (intensification) to obtain the expected maximum return. On the other hand, it is also necessary to choose different actions to explore other policies (diversification). The ϵ -Greedy policy consists of a good strategy to balance intensification and diversification, choosing the action with the highest value in Q with probability $1 - \epsilon$ or selecting an action at random with probability ϵ . The Q-table represents the learning process with the value of each state-action pair.

In our implementation, at the end of each BRKGA-QL generation j, a reward $R^{i}(s, a)$ is incremented for the corresponding state-action pair (s, a) and Q-table i, as showed by Equation (2), where $\delta_{b_{j}}$ is the best fitness in the current generation and $\delta_{b_{j-1}}$ the previous one.

$$R^{i}(s,a) \leftarrow R^{i}(s,a) + \begin{cases} \frac{(\delta_{b_{j-1}}/\delta_{b_{j}})-1}{|P|}, & \text{if } \delta_{b_{j}} < \delta_{b_{j-1}} \\ 0, & \text{otherwise} \end{cases}$$
 (2)

Furthermore, the reward function serves as an intermediary solution, striking a balance between enhancing the current best fitness and the binary rewards as proposed by Karafotias et al. (2015). Notably, this function exhibits a higher sensitivity to scale than the binary reward, considering the magnitude of improvement and the population size. Table 3 presents the potential states for each parameter, with λ^{df} fixed as 0.8 and λ^{lf} starts with 1 and decreases linearly until 0.1 at the time limit. The Q-table initially has all values set to 0. It undergoes updates every k BRKGA-QL generation using Equation (1), followed by the reset of corresponding rewards.

Table 3: Possible parameter states.

Parameter	States
P	233, 377, 610, 987, 1597, 2584
p_e	0.10, 0.15, 0.20, 0.25, 0.30
μ	0.01,0.02,0.03,0.04,0.05
$ ho_e$	0.55, 0.60, 0.65, 0.70, 0.75, 0.80

Finally, Algorithm 8 presents the summarised implementation of the BRKGA-QL. It is comprised of a usual BRKGA implementation (Gonçalves and Resende, 2011) coupled with a local search (Lines 16–19) and the added QL component (Lines 1, 5, 6 and 15). The point of integration between the problem at hand (IORSP) and BRKGA implementations, including the present one, lies in the decoder function. This function receives an individual (a vector of random keys) and deterministically maps it into a feasible solution, a process that is elaborated upon in the section 4.5.

```
Algorithm 8: BRKGA-QL
   Input: Time limit TL
   Output: Best solution found A^{best}
 1 Step 1: Initialize Q-Table values;
 2 Step 2: Randomly generate the population P;
 3 Step 3: Evaluate and sort P by fitness. Store the best individual in A^{best};
   while TL is not reached do
       Step 4: Set Q-Learning parameters (\epsilon, lf, df);
 6
      Step 5: Choose an action for each parameter (p, p_e, \mu, \rho_e) from the Q-Table using the
        \epsilon-greedy policy;
       Step 6: Evolutionary process;
 7
       Classify P as elite or non-elite individuals;
 8
       Create elite set P_e using p_e as a guide;
 9
       Create the offspring set P_c through the blending procedure, using \rho_e, \mu, and
10
        factor = 1 as guides;
       P \leftarrow P_e \cup P_c;
11
       Evaluate and sort P by fitness;
12
      if the best individual improved then
13
          Store the best individual in A^{best};
14
          Step 7: Set reward (R^i) and update Q-Table;
15
      if exploration or stagnation is detected then
16
          Step 8: Local Search;
17
          Identify communities in P_e with the clustering method;
18
          Apply RVND in the best individuals of these communities;
19
          Apply Shaking in other individuals;
20
21 return A^{best}:
```

4.3. Simulated Annealing

Simulated Annealing (SA) is a widely used global optimization method inspired by statistical physics Kirkpatrick et al. (1983); Černý (1985) and is supported by theoretical guarantees of global convergence Dekkers and Aarts (1991). SA starts with an initial solution (denoted as a vector of random keys) $A \in S$, where S represents the random-key solution space. Then, a neighbourhood solution A' is generated through a perturbation algorithm. The search procedure in SA is based on the Metropolis acceptance criterion of Metropolis et al. (1953), which models how a thermodynamic system moves from the current solution (state) to a candidate solution in which the objective function (energy content) is being minimised. If $\delta_{\mathscr{D}(A')} - \delta_{\mathscr{D}(A)} \leq 0$, then A' is accepted as the current solution, else the candidate solution is accepted based on the acceptance probability:

$$P(A') = \exp\left(-\frac{\Delta E}{T}\right),\tag{3}$$

where $\Delta E = \delta_{\mathscr{D}(A')} - \delta_{\mathscr{D}(A)}$ and T defines the current temperature. The key idea is to prevent the algorithm from becoming trapped in local optima by allowing uphill moves. It is important to note that uphill moves are more likely to occur at higher temperatures.

Algorithm 9 presents the SA pseudo-code used in this work. The procedure starts by initializing with a solution represented by a random-key vector A. The algorithm runs a loop until a stopping criterion is met. Within this loop, it generates a neighboring solution (A') from the current solution (A) and calculates the difference in objective function values (energy difference, ΔE).

If the new solution has a lower energy ($\Delta E \leq 0$), it is accepted as the current solution and potentially updates the best-found solution. If the new solution has higher energy ($\Delta E > 0$), it may still be accepted based on a probability determined by the Metropolis criterion via Equation (3), which allows for occasional uphill moves to escape local optima. The temperature (T) is then updated by multiplying it with a cooling rate (α). An RNVD is subsequently called to refine the current solution further. This process continues, gradually reducing the temperature and thus the probability of accepting worse solutions until the stopping criterion is satisfied. The algorithm finally returns the best solution found during the search.

Algorithm 9: Simulated Annealing

```
Data: Random-key vector A, initial temperature T_0, cooling rate \alpha, \beta_{min}, \beta_{max}, SA_{max},
                time limit TL
     Result: Best found solution
 1 A^{best} \leftarrow A, T \leftarrow T_0;
    while TL is not reached do
          iter \leftarrow 0;
 3
          while iter < SA_{max} do
 4
                A' \leftarrow \text{Shaking}(A, \beta_{min}, \beta_{max});
 5
                Calculate the energy difference \Delta E \leftarrow \delta_{\mathscr{Q}(A')} - \delta_{\mathscr{Q}(A)};
 6
                if \Delta E \le 0 then
 7
                     A \leftarrow A';
  8
                     \begin{array}{l} \textbf{if} \ \delta_{\mathscr{D}(A)} < \delta_{\mathscr{D}(A^{best})} \ \textbf{then} \\ \mid \ A^{best} \leftarrow A; \end{array}
  9
10
                else
11
                     Calculate the acceptance probability P \leftarrow \exp\left(-\frac{\Delta E}{T}\right);
12
                     Generate a random number r \in [0, 1];
13
                     if r < P then
14
                       A \leftarrow A';
15
               iter + +;
16
          Update temperature T \leftarrow \alpha \times T;
17
          A \leftarrow \text{RVND}(A);
18
19 return A^{best}
```

4.4. Iterated Local Search

The Iterated Local Search (ILS) is a straightforward yet powerful heuristic to solve various optimization problems. The foundational idea of ILS was introduced by Baxter (1981) and further elaborated by Lourenço et al. (2003). The essence of ILS lies in iteratively constructing a sequence of solutions using a specific heuristic, which typically leads to significantly better solutions than repeated random trials of the same heuristic. This optimization technique attempts to escape local optima by applying local search and perturbation in an iterative manner.

The ILS algorithm, as detailed in Algorithm 10, begins with a random-key vector A as input. Initially, the vector A undergoes an RVND process, resulting in the solution set as A^{best} . The algorithm then enters a loop until the stopping criterion is met. A copy of A^{best} , denoted as A', is created and perturbed within the loop. This perturbed solution is then refined using the RVND function. If the objective function value $\delta_{\mathcal{D}(A')}$ of the newly obtained solution A' is better than that of the current best solution A^{best} , represented as $\delta_{\mathcal{D}(A^{best})}$, then A^{best} is updated to A'. Once the stopping criterion is satisfied, the algorithm returns A^{best} as the best-found solution.

Algorithm 10: Iterated Local Search

```
Data: Random-key vector A, \beta_{min}, \beta_{max}, time limit TL

Result: Best found solution

1 A \leftarrow \text{RVND}(A);

2 A^{best} \leftarrow A;

3 while TL is not reached do

4 A' \leftarrow A^{best};

5 A' \leftarrow \text{Shaking}(A', \beta_{min}, \beta_{max});

6 A' \leftarrow \text{RVND}(A');

7 if \delta_{\mathcal{D}(A')} < \delta_{\mathcal{D}(A^{best})} then

8 A^{best} \leftarrow A';

9 return A^{best};
```

4.5. Encoding and Decoding

Solutions to the IORSP are encoded with a vector A of n = |K| random keys, where K is the set of surgeries. Then, each random key corresponds to a unique surgery. Our decoder implementation follows a straightforward approach: i) sorts the surgeries based on their random-key values, ii) sorts the surgeries based on their priority values, keeping the random-key order for equal priorities; iii) schedules each surgery task sequentially at the earliest available time slots.

Table 4 shows the decoder's dynamic structures and operators. We have a solution problem s_A that contains, for each surgery $k \in K$, a surgery allocation data D_k , and each surgery allocation data contains an allocated room r_k , set of equipment e_t , starting time σ_t and blocking time ψ_t . Thus, the scheduled surgeries makespan $\delta_{\mathcal{D}(A)}$ is when the last patient completes its last task.

Table 4: Decoder Notations										
Solution variables										
s_A	Solution problem construct from random-key vector A									
D_k	Surgery's k allocation data									
r_t	Room for task t									
e_t	Set of equipment for task t									
σ_t	Starting time for task t									
ψ_t	Blocking time for task t									
$\delta_{\mathscr{D}(A)}$	Makespan of random-key vector A									
Operators										
Next(t)	Returns the next task to be executed after t on the same surgery									
First(k)	Returns the first task to be executed on surgery k									
Last(k)	Returns the last task to be executed on surgery k									
$Search(R_t, k, s_A, \sigma^{min})$	Returns the earliest available resource r and the corresponding candidate									
	moment σ_r^c at which task k can be executed in solution s_A , after moment σ^{min} .									

Algorithm 11 details our implementation. The solution starts with no surgeries scheduled (Line 1) and, consequently, $\delta_{\mathcal{D}(A)} = 0$, then the surgeries are sorted given the sequence of random keys (Line 2). Then, given the final sequence of surgeries, each one is scheduled by our Greed Insertion algorithm (Line 4).

Algorithm 12 details the Greed Insertion algorithm. It also has the simple concept of scheduling each surgery's task as soon as possible, given all available rooms, types of equipment, and persons. It receives a current problem solution s_A and a surgery k to be scheduled and starts by setting variable σ^m (minimal start time) to zero and Success to false (Line 1). The main loop (Lines 2–22), for each task (Line 4), searches all compatible rooms R_t and selects it the one r_t with the earliest moment available σ_c (Line 6), with the assistance of operator Search as noted on Table

Algorithm 11: Decoder

```
Data: Vector A of random keys
Result: Fitness (makespan) value, \delta_{\mathscr{D}(A)}

1 s_A \leftarrow \emptyset; \delta_{\mathscr{D}(A)} \leftarrow 0;
2 SortByRK(A);
3 for a \in A do
4 \bigcup GreedInsertion(s_A, K_a, \delta_{\mathscr{D}(A)});
5 return \delta_{\mathscr{D}(A)}
```

4. The same logic is applied to select the required equipment types F_t , if any is required (Lines 9–12) and for the required people P_t (Lines 13–15).

Variable σ_t indicates the selected start time for task k. It starts as σ^{min} (Line 5), and it is updated with the maximum value of the selected room (Line 7), each selected equipment (Line 12) and each involved person's schedule (Line 15). The blocking value ϕ_t is computed as the delay (Line 16), if it exceeds the limit (Line 17), the new σ^{min} is set by delaying the first task (Line 18) and restarting k's scheduling (Line 19), otherwise σ^{min} is updated to allocate the following task (Line 21). After a successful surgery allocation, the surgery allocation data D_k is added to solution s_A (Line 23) and hence, the makespan $\delta_{\mathcal{D}(A)}$ is updated (Line 24).

Algorithm 12: Greed Insertion

```
Data: Solution s_A, surgery k, and the current makespan \delta_{\mathscr{D}(A)}
      Result: A Solution s_A with surgery k scheduled.
  1 \sigma^m \leftarrow 0; Success \leftarrow False;
      while \neg Success\ \mathbf{do}
              Success \leftarrow True; D_k \leftarrow \emptyset;
  3
              for Task \ t \in T_k do
  4
                     \sigma_t \leftarrow \sigma^{min}:
  5
                     (r_t, \sigma^c) \leftarrow Search(R_t, t, s_A, \sigma_t);
  6
                     \sigma_t \leftarrow max(\sigma_t, \sigma^c);
  7
                     e_t \leftarrow \emptyset;
  8
                     for f \in F_t do
  9
                            (e, \sigma^c) \leftarrow Search(E_f, t, s_A, \sigma_t);
 10
                            e_t \leftarrow e_t \bigcup \{e\};
 11
                         \sigma_t \leftarrow max(\sigma_t, \sigma^c);
 12
                     for p \in P_t do
 13
                            (p, \sigma^c) \leftarrow Search(\{p\}, t, s_A, \sigma_t);
 14
                            \sigma_t \leftarrow max(\sigma_t, \sigma^c);
 15
                     \phi_t \leftarrow \sigma_t - \sigma^{min}:
 16
                     if \phi_t > \Phi then
 17
                            \sigma^{min} \leftarrow \sigma_{First(k)} + \phi_t;
 18
                            Success \leftarrow False; Break;
 19
 20
                       \sigma^m \leftarrow \sigma_t + \gamma_t^d + \gamma_t^m;
 21
                     D_k \leftarrow D_k \bigcup \{(r_t, e_t, \sigma_t, \phi_t)\};
23 s_A \leftarrow s_A \bigcup \{D_k\};
24 \delta_{\mathscr{D}(A)} \leftarrow max(\delta_{\mathscr{D}(A)}, \sigma_{Last(k)} + \gamma_{Last(k)}^d);
```

Figure 5 illustrates an example of the Algorithm 11 on a simplified scenario with five surgeries, no priorities, two beds, two ORs, one PSRU, and all subjects with clear initial schedules. Notably, Surgeries 2 and 3 lack PSRU tasks; not all tasks follow the same room sequencing, and all surgeries allocate first and last the same bed as described in Section 1.

The decoder receives a vector of random keys $A = \{0.2, 0.6, 0.1, 0.4, 0.3\}$. Subsequently, each

surgery is scheduled in the sequence 3, 1, 5, 4, and 2. Firstly, Surgery 3 involves 3 tasks, with the first task allocating Bed 1 at the first time slot, OR 1 at the second time slot, and the patient returning to Bed 1 at the third time slot. Surgery 1 comprises 4 tasks, with the first allocating Bed 1 at the first time slot, OR 2 at the second and third time slots, the PSRU at the fourth, and the patient returning to Bed 2 at the fifth. Similarly, Surgeries 5, 4, and 2 also have their respective tasks sequentially allocated at the first available moment.

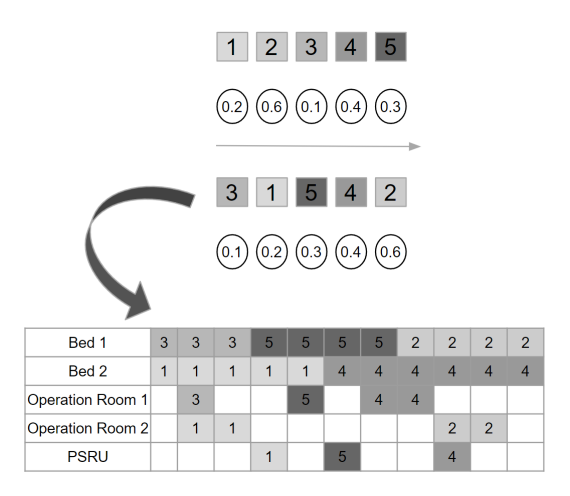


Figure 5: Example of our decoder with a Greed Insertion strategy.

5. Computational experiments and analysis

Our proposed metaheuristics were coded in C++ and compiled with GCC. The proposed lower bound models were coded on Python and solved with Gurobi 10.01 (Gurobi Optimization, LLC, 2023). The computer used in all experiments was a Dual Xenon Silver 4114 20c/40t 2.2Ghz processor with 96GB of DDR4 RAM and running CentOS 8.0 x64. Each proposed model was solved for each instance with a time limit of 3600 seconds, and the metaheuristics were run five times for each instance with a time limit proportional to the number of surgeries. The literature instances and results were retrieved from Burdett and Kozan (2018), and our case study instances were generated based on gathered data from multiple sources. This process is detailed in Section 5.2. Table 5 presents the general characteristics of each instance, with its name, number of surgeries and number of rooms per room type in the sequence a patient usually has, and the total CPU time limit (TL) of each heuristics run.

The parameters of the SA and ILS are tuned using an offline strategy. We applied an experimental design approach considering potential values for each parameter and identifying the "best" value for each parameter through many experiments on a subset of the problem instances. The parameters of the ILS were $\beta_{min} = 0.10$ and $\beta_{max} = 0.20$. The parameters of the SA were $T_0 = 1000000$, $\alpha = 0.99$, $SA_{max} = 200$ $\beta_{min} = 0.05$, and $\beta_{max} = 0.20$. The parameters of the BRKGA-QL are tuned during the search process using the Q-Learning method.

We analyzed the computational results in terms of quality and robustness. We present the average CPU time and the relative percentile deviation (RPD) for the best solution found (X_{min}) as shown in Equation 4. The RPD values are relative deviations from reference ones. We calculated the RPD in each run and presented the average and best values. A statistical analysis is made per table between the resulting average RPDs. First, we classify it as parametric or non-parametric and then compare it with the Paired T Student Test group, if parametric, or with the Wilcoxon test otherwise. The algorithms are compared in pairs with the null hypothesis first; if rejected,

Table 5: Literature and case study instances details.

	Literature		Case Study					
Name	#Surgeries	#Rooms	TL(s)	Name	#Surgeries	#Rooms	TL(s)	
CASE_01.dat	50	5,2,5,10	120	p070	58	31,3,2,4	60	
$CASE_02.dat$	100	5,2,5,10	200	p078	66	23,3,3,4	70	
$CASE_03.dat$	150	5,2,5,10	240	p087	75	29,3,3,4	80	
$CASE_04.dat$	200	5,2,5,10	300	p093	81	30,3,3,4	90	
$CASE_05.dat$	50	5,3,5,10	120	p098	86	40,3,2,4	100	
$CASE_06.dat$	100	5,3,5,10	200	p100	84	39,4,3,5	100	
$CASE_07.dat$	150	5,3,5,10	240	p109	93	35,4,3,5	100	
CASE_08.dat	200	5,3,5,10	300	p120	104	46,4,4,5	100	
CASE_09.dat	50	5,4,5,20	120	p138	118	43,5,4,5	120	
$CASE_10.dat$	100	5,4,5,20	200	p153	133	71,5,4,7	120	
CASE_11.dat	150	5,4,5,20	240	p165	141	78,6,4,7	130	
$CASE_12.dat$	200	5,4,5,20	300	p178	154	88,6,4,6	130	
$CASE_13.dat$	50	5,5,5,20	120	p183	159	89,6,4,6	140	
$CASE_14.dat$	100	5,5,5,20	200	p189	161	71,7,5,7	140	
$CASE_15.dat$	150	5,5,5,20	240	p192	164	72,7,4,8	140	
$CASE_16.dat$	200	5,5,5,20	300	p193	165	78,7,5,7	140	
$CASE_17.dat$	50	5,10,5,20	120	p197	173	99,6,5,7	160	
CASE_18.dat	100	5,10,5,20	200	p201	177	73,6,4,8	160	
$CASE_19.dat$	150	5,10,5,20	240	p216	188	95,7,5,9	160	
$CASE_20.dat$	200	5,10,5,20	300	p233	197	88,9,4,10	160	
CASE_21.dat	50	5,10,5,30	120					
$CASE_22.dat$	100	5,10,5,30	200					
$CASE_23.dat$	150	$5,\!10,\!5,\!30$	240					
CASE_24.dat	200	5,10,5,30	300					

the "less" alternative hypothesis is tested, and superior performance is considered given statistical confidence greater than 95% (p-value ≤ 0.05).

$$RPD = (X/X_{min} - 1) \times 100 \tag{4}$$

5.1. Computational results for literature instances

The case study modelling of Burdett and Kozan (2018) does not completely match ours. The main difference is that, in their case, the wardroom is the long-time recovery room; in our case, the patient returns to the initial bed for a long recovery. In both cases, one type of room is reserved during each patient's whole stay. This allowed their case to be compatible with Formulation (A.1)-(A.5). For these instances, the distinction between the scenarios with and without business hours lies in the fact that, in the case with it, the ORs are only operational during regular business hours (from 8:00 AM to 5:00 PM from Monday until Friday), and the other rooms are always available, these are implemented with availability slots. Other distinctions include the absence of surgeon or equipment scheduling, compatibility between rooms and surgery types, and customisation in initial schedules. These variances were more straightforward to accommodate when we examined a simplified scenario based on our case study. In the following tables, the displayed lower bounds are the best ones computed by any of our relaxed formulations; the formulations and their results are detailed on Appendix A-Appendix C.

Table 6 shows our heuristic results with the literature instances without business hours. The old lower bound and Hybrid Simulated Annealing (HSA) results are reported from Burdett and Kozan (2018), algorithms were coded on C++ and ran on a personal computer with a 2.6Ghz processor and 16GB of RAM under Windows 7. The first tree columns describe the instances, followed by the literature lower bound (Old), our best computed lower bound from Table C.9 (New), followed by the HSA and RKO heuristic results, the makespan values for best solution found (best) in days, its best and average relative percentile deviation, respectively BRPD and ARPD, and the average time to the best solution (ATTB) in seconds. Analysing the results, our

relaxed formulations computed lower bound values better than the ones in the literature. Besides, the RKO methods found better results for all literature instances without business hours. The SA found seven new best-known solutions (BKS), the ILS found 15 new BKS, and the BRKGA-QL found four new BKS. These methods are robust with very small RPDs. The statistical tests concluded that all RKO heuristics performed better than the literature heuristic, and between the RKO heuristics, the ILS was superior to the other two (p-values return by the Wilcoxon test were 7.35E-11 between ILS and BRKGA-QL and 0.0013 between ILS and SA), and the SA was superior to the BRKGA-QL (p-value was 4.13E-08). The ATTB shows us that the BRKGA-QL was the fastest to converge to the best solution found. Looking at the obtained new lower bounds and upper bounds, instance "CASE_21" has an optimal result proved, and such a solution was found by all three RKO heuristics.

<u>Table 6: Literature instances heuristic results without business hours</u> BRKGA-QI BRPD(BRPD(%) Old ARPD(% ATTB(s) CASE_01 14.82 16.41 16.80 1.54 172.8 16.55 0.00 16.55 0.04 60.03 16.56 0.07 0.11 33.76 CASE_02 145.74 35.44 32.24 35.32 36.04 1.73 1821.6 35.43 0.02 136.49 35.43 0.05 20.56 0.04 0.00 0.02 0.07 CASE_03 49.19 0.004 206.45 49.19 149.66 43.57 49.06 50.10 6282 0.01 0.00 0.01 49.19 0.004 0.02 CASE_04 60.81 67.05 68.13 1.43 16110 67.17 0.001 0.02 247.83 67.17 0.00 0.01 240.66 67.18 0.02 0.04 101.91 CASE_05 16.88 17.41 2.70 151.2 16.95 0.00 0.02 67.31 16.95 0.004 0.03 73.97 0.07 0.02 CASE 06 29.89 32 94 34 49 4.47 1605.6 33.02 0.01 0.02 89 23 0.00 116.35 33.03 0.04 0.08 53.68 33.01 CASE_07 44.18 48.81 49.45 1.17 6080.4 48.88 0.01 0.03 147.67 48.88 0.00 0.01 172.58 48.89 0.02 0.04 71.14CASE_08 61.27 67.50 68.73 1.72 11998.8 67.57 0.00 0.01 161.91 67.57 0.002 0.01 208.13 0.01 0.03 93.41 CASE 09 6.79 7.60 8.17 5.82 122.4 7.73 0.11 0.14 87.15 7.73 0.13 0.20 113.37 7.72 0.00 0.33 42.76 CASE_10 17.54 14.99 5.13 16.69 0.02 0.07 16.68 0.06 110.71 0.06 126.59 16.531396.8 146.130.00 16.69 0.15CASE_11 22.09 24.31 25.95 5230.8 189.41 0.04 140.09 56.42 CASE_12 30.57 33.60 35.13 4.12 12834 33.74 0.00 0.05 207.66 33.75 0.02 0.06 251.78 33.75 0.04 0.09 114.96 CASE_13 10.47 76.66 0.17 8.23 9.08 118.8 0.00 0.26 CASE_14 15.41 16.92 18.72 9.76 1317.6 17.06 137.33 17.06 114.33 17.06 48.61 0.04 0.06 0.00 0.02 0.03 0.14 CASE_15 23.31 25.5027.11 5.82 4788 25.63 0.02 0.07 152.1425.62 0.00 0.05 120.20 25.64 0.09 0.15 129.74 CASE_16 4.58 12394.8 289.84 35.40 32.23 37.02 35.41 0.03 0.04 226.79 0.004 0.04 0.00 0.04 188.69 CASE_17 9.03 9.79 7.66 97.2 9.09 0.00 0.16 82.16 9.12 0.31 66.70 9.12 0.30 0.41 81.80 8.23 0.30 CASE_18 15.46 16.99 18.22 6.74 1202.4 17.08 0.03 0.07 164.61 17.07 0.00 0.06 116.01 17.07 0.02 0.13 52.89 CASE_19 0.04 0.09 0.05 226.69 0.03 CASE_20 30.48 33.55 35.29 4.95 11134.8 33.65 0.06 0.08 284.51 33.63 0.00 0.03 212.56 33.63 0.01 0.08 135.85 CASE_21 5.04 6.09 6.54 7.36 6.09 0.00 0.00 45.72 0.00 0.02 34.39 6.09 0.00 0.08 59.23 118.8 6.09 CASE_22 10.02 12.31 1220.40.00 0.21 153.65 0.12 137.17 11.21 0.14 116.34 CASE_23 14.18 15.70 17.31 9.27 4356 15.86 0.11 0.21 222.80 15.87 0.15 0.18 197.95 15.84 0.00 0.12 163.00 263.55 CASE_24 23.027.51 10875.6 21.42 0.04 0.15 0.00 0.08 269.12 0.03 0.13 167.0221.2621.4121.42

Table 7 shows our heuristic results with the literature instances with business hours. Similar to the previous table, the HSA results are reported from Burdett and Kozan (2018) with its solution times in seconds, makespan values for the best solution found (best) in days, its best and average relative percentile deviation, respectively BRPD and ARPD, and the average time to best (ATTB) in seconds. Upon analysis of the results, we observed that the RKO methods consistently enhanced the results for all instances from the literature. Specifically, SA found eight new best-known solutions (BKS), ILS found two new BKS, and BRKGA-QL found 18 new BKS. Statistical tests confirm that all RKO heuristics demonstrated superior performance compared to the HSA, as shown in Table 6. An inverse performance order was observed among the RKO heuristics: BRKGA-QL outperformed the other two methods (Wilcoxon test p-values: 3.08E-08 when compared to SA, and 3.45E-10 when compared to ILS). No statistically significant difference was found between ILS and SA (p-value: 0.0528). Notably, the disparity between the ARPDs was more pronounced than in Table 6.

Figure 6 presents the performance profile proposed by Dolan and Moré (2002), considering the RKO-based heuristics for BRKGA-QL, SA, and ILS, with a gap limit of 1% relative to the best-known solutions (BKS) for each of the tested instances. When the performance ratio is zero, BRKGA-QL attains the best gaps for 80% of the solved instances, ILS achieves the best gaps for 16% of the instances, and SA achieves the best gaps for only 4% of the solved instances. When the performance ratio is increased to 2 (x-axis = $log_2(2) = 1$), BRKGA-QL solves 95% of the instances with the best gaps, while ILS and SA solve 50% and 46% of the instances, respectively. As higher performance ratios are allowed, the percentage of instances solved with gaps smaller

Table 7: Literature instances heuristic results with business hours.															
	HSA SA				ILS				BRKGA-QL						
Instance	best	BRPD(%)	time (s)	best	BRPD(%)	ARPD(%)	ATTB(s)	best	BRPD(%)	ARPD(%)	ATTB(s)	best	BRPD(%)	ARPD(%)	ATTB(s)
CASE_01	19.63	11.83	900	17.55	0.00	1.41	105.88	18.29	4.19	4.22	85.10	18.24	3.91	4.13	63.02
CASE_02	42.19	10.01	9432	39.35	2.61	2.77	182.27	38.51	0.42	1.91	166.37	38.35	0.00	1.58	128.39
CASE_03	59.33	3.45	32796	57.35	0.00	0.97	166.53	57.40	0.09	1.13	197.60	57.42	0.12	0.84	152.11
CASE_04	79.46	1.15	110160	79.39	1.06	2.13	261.99	79.33	0.98	1.69	239.34	78.55	0.00	1.15	170.95
CASE_05	20.01	13.42	828	17.64	0.00	0.26	83.20	17.65	0.02	2.48	68.14	17.69	0.29	2.83	62.50
CASE_06	38.59	9.02	8100	36.65	3.53	3.73	148.24	36.71	3.71	3.87	82.74	35.40	0.00	2.68	127.25
CASE_07	56.85	8.48	32652	54.16	3.35	4.55	165.40	53.35	1.80	3.24	168.99	52.40	0.00	1.83	164.81
CASE_08	68.41	1.25	13572	67.57	0.00	0.01	263.05	67.57	0.001	0.01	232.98	67.57	0.01	0.02	49.77
CASE_09	10.06	16.18	576	8.66	0.00	0.00	78.00	8.66	0.00	1.17	66.21	8.66	0.00	0.97	69.93
CASE_10	20.52	15.76	6120	18.43	3.98	4.59	163.51	18.38	3.69	4.22	145.38	17.73	0.00	3.53	88.51
CASE_11	32.08	21.38	24480	27.55	4.24	9.06	195.44	27.38	3.61	7.76	151.45	26.43	0.00	0.86	162.70
CASE_12	42.34	9.95	76464	39.50	2.57	4.41	246.59	38.81	0.79	2.00	271.43	38.51	0.00	1.53	281.31
$CASE_13$	11.65	28.89	504	9.04	0.00	1.69	86.49	9.34	3.32	3.96	51.51	9.34	3.32	3.33	71.88
CASE_14	21.41	16.68	5760	18.38	0.17	0.72	139.00	18.36	0.06	0.54	143.49	18.35	0.00	0.38	97.93
$CASE_15$	32.74	19.31	24012	29.39	7.10	7.30	174.32	29.34	6.92	7.22	165.69	27.44	0.00	1.33	208.53
CASE_16	44.43	10.39	69624	40.99	1.83	2.45	299.90	40.34	0.23	1.09	293.65	40.25	0.00	0.32	269.92
$CASE_17$	11.73	18.02	432	9.94	0.00	2.24	80.73	10.25	3.08	3.66	48.44	10.12	1.87	2.85	59.19
CASE_18	20.47	11.87	4716	18.44	0.79	0.95	175.08	18.41	0.59	0.81	189.10	18.30	0.00	0.37	106.51
CASE_19	33.41	18.00	20700	29.42	3.90	4.34	183.18	29.37	3.73	3.95	203.83	28.31	0.00	1.89	178.83
CASE_20	41.87	14.34	59904	37.53	2.47	4.53	267.41	37.53	2.48	4.34	269.61	36.62	0.00	2.48	223.29
$CASE_21$	7.88	22.08	360	6.45	0.00	0.16	69.78	6.45	0.00	0.31	36.21	6.45	0.00	0.06	51.74
$CASE_22$	15.15	22.36	4500	12.71	2.64	4.88	128.54	12.50	0.94	2.70	183.73	12.38	0.00	0.60	126.03
CASE_23	22.12	25.23	17928	18.33	3.80	4.79	218.44	18.32	3.72	4.06	204.68	17.66	0.00	2.37	190.68
CASE_24	27.36	12.32	56124	25.23	3.56	4.89	304.89	24.52	0.67	3.23	267.27	24.36	0.00	1.52	264.02
Averages		14.22	24193.50		1.98	3.03	174.49		1.88	2.90	163.87		0.40	1.64	140.41

than 1% remains constant for BRKGA-QL at 95%. In contrast, ILS and SA can solve 79% and 70% of the instances, respectively.

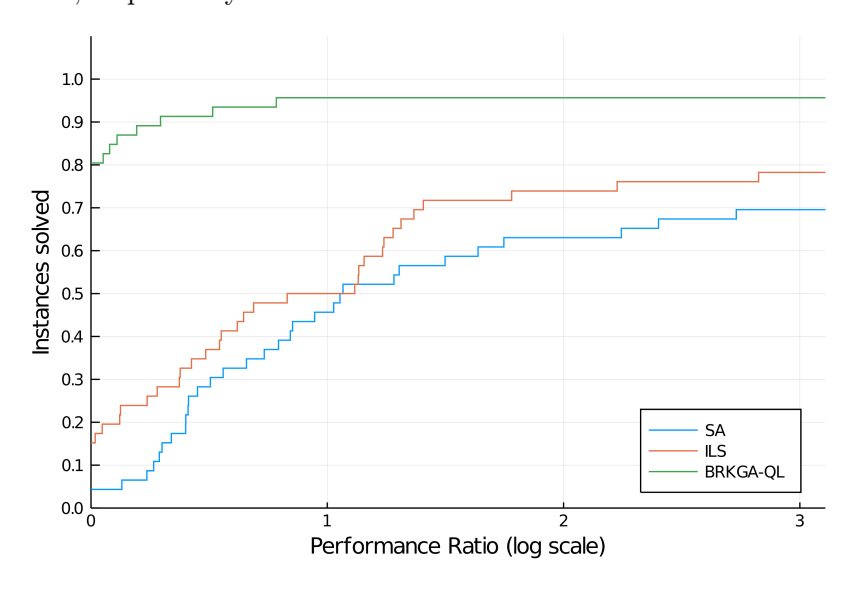


Figure 6: Performance Profile considering the RKO-based heuristics.

The Time To Target (TTT) plot, as described in Aiex et al. (2007), is used to analyze the RKO convergence rate considering BRKGA-QL, SA, and ILS heuristics. The instance set fjsp-nostr/CASE_21 was considered for this test. All three solution procedures find the same solution, which is also the best-known solution for this instance. The experiment consists of running each method 100 times for the instance. Each run is independent and stops when a solution with a cost at least as good as a given target value is found. These experiments consider an integer value at most 0.50% greater than the BKS solution as the target. The analysis of Figure 7 indicates that within the first 20 seconds, BRKGA-QL has a 97% probability of reaching the target value, compared to 93% for ILS and 44% for SA. By 40 seconds, BRKGA-QL consistently achieves the target value, while ILS and SA reach probabilities of 98% and 89%, respectively. The likelihood of reaching the target increases to 100% at approximately 50 seconds for ILS and 58 seconds for SA. These results demonstrate that while all three methods exhibit strong convergence, BRKGA-QL

achieves the fastest convergence.

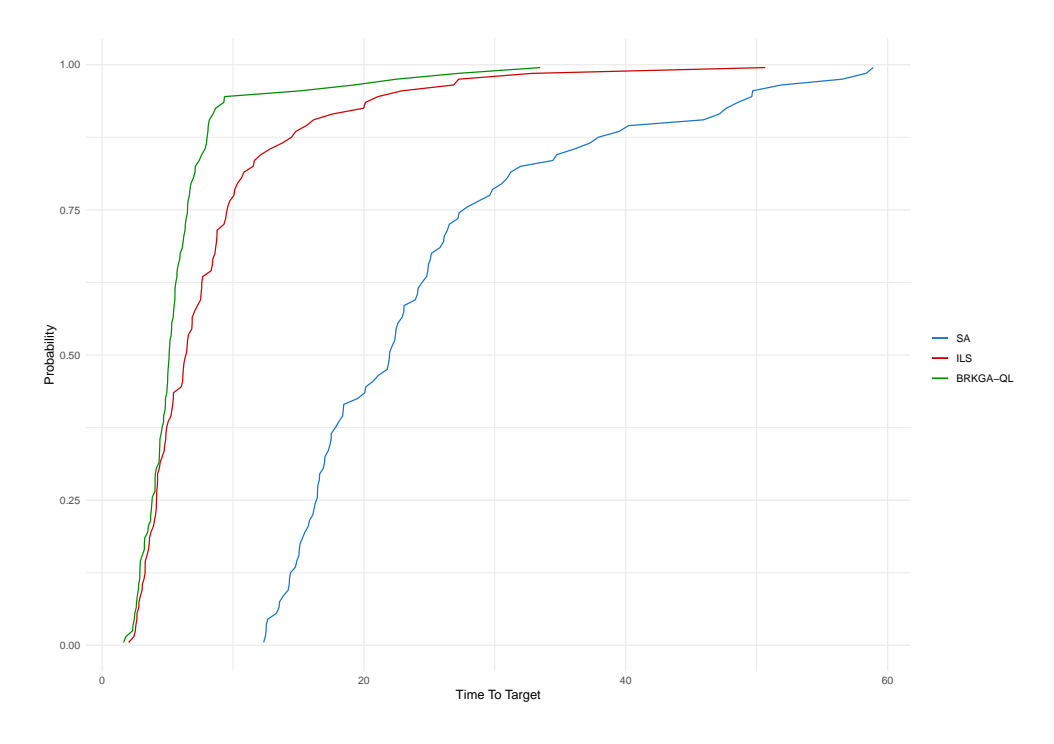


Figure 7: Time to target plot (Instance fjspnostr/CASE_21)

Based on the computational tests, no single method outperformed the others in all cases. Therefore, we selected the BRKGA-QL method for the case study, as it provided better results for instances considering business hours. Additionally, this method does not require offline parameter tuning, making it more convenient for day-to-day hospital management. The case study instances are more complex and constrained by factors such as surgeon schedules, operating room types, equipment availability, and other additional attributes.

5.2. Computational results for the case study instances

Our case study instances were primarily generated using data collected from Santa Casa, a non-profit hospital with locations in several cities across Brazil. The surgery types, operating times, and probability distribution functions for occurrence were sourced from Costa (2017) and Siqueira et al. (2018a). The script initially receives or randomly picks some surgeries, multiplies per a constant, and picks a number inside a $\pm 15\%$ range for the number of surgeons, number of each room type, and available types of equipment. For a 14-day planning horizon, operating rooms and surgeons are only available from 7:00 AM to 10:00 PM. The other room types are always available. Each day, a surgeon is available with a 70% chance. Based on our case study collected data, each operating room is always available from Monday to Friday and from 7:00 AM to 1:00 PM on Saturdays with a 35% chance. The equipment requirement is determined according to the surgery type. The generated set of instances is publicly available at a Github repository.

Table 8 shows our heuristic results with the case study instances. The first tree columns describe the instances, followed by the best computed lower bound from Table C.10, followed by the BRKGA-QL results split between the cases with and without availability slots (AS). For these instances, the tests without availability slots imply that all subjects (rooms, surgeons, patients, or equipment) are always available. Each instance has the best and average makespan value in days and the average CPU time in seconds. The case with no availability slots has a percentile optimality gap comparing the best solution to the best lower bound.

Analysing the gap results, eight instances had gaps smaller than 1%, even among the larger ones. This shows that the BRKGA-QL found almost optimal results even in instances with many more constraints (surgeon schedules, OR compatibility, and equipment availability) in relation to the instances of (Burdett and Kozan, 2018). BRKGA-QL demonstrated the ability to identify high-quality solutions within seconds of computation time, even for large-scale instances containing approximately 200 surgical procedures. The algorithm was executed 15 times for each instance, exhibiting robust performance by consistently producing average solutions close to the best solutions obtained. These attributes make BRKGA-QL suitable for practical implementation in hospital management systems, where computational efficiency and solution quality are essential.

Table 8: Case study instances heuristic results.

				BRKGA-QL								
						No AS				W	ith AS	
Instance	Surgeries	Rooms	Best LB	Best	Average	ARPD(%)	Time(s)	Gap (%)	Best	Average	ARPD(%)	Time(s)
p070	58	31,3,2,4	4.44	4.61	4.632	0.48	60.1	3.85	6.615	6.96	5.22	60.1
p078	66	23,3,3,4	5.536	6.057	6.073	0.26	70.1	9.41	8.959	9.036	0.86	70.4
p087	75	29,3,3,4	5.247	5.679	5.698	0.33	80.1	8.23	9.663	9.678	0.16	80.1
p093	81	30,3,3,4	5.485	5.848	5.87	0.38	90.1	6.62	9.678	9.706	0.29	94.4
p098	86	40,3,2,4	5.719	5.728	5.731	0.05	100.1	0.15	9.648	9.675	0.28	104.6
p100	84	39,4,3,5	4.604	4.981	4.998	0.34	100.1	8.19	8.708	8.74	0.37	104.9
p109	93	35,4,3,5	5.364	5.926	5.942	0.27	100.1	10.47	9.534	9.57	0.38	103.7
p120	104	46,4,4,5	5.466	5.497	5.515	0.33	100.2	0.57	9.823	9.876	0.54	105
p138	118	43,5,4,5	5.224	5.776	5.801	0.43	120.2	10.55	9.252	9.315	0.68	126
p153	133	71,5,4,7	5.486	5.503	5.515	0.22	120.2	0.3	9.994	10.115	1.21	124.9
p165	141	78,6,4,7	5.019	5.042	5.055	0.26	120.3	0.46	9.233	9.257	0.26	131.3
p178	154	88,6,4,6	5.335	5.353	5.369	0.30	120.3	0.34	9.901	10.026	1.26	128.8
p183	159	89,6,4,6	5.556	5.588	5.596	0.14	140.4	0.56	10.344	10.528	1.78	146.2
p189	161	71,7,5,7	4.902	5.238	5.278	0.76	140.4	6.86	8.847	8.934	0.98	140.3
p192	164	72,7,4,8	4.964	5.257	5.28	0.44	140.4	5.9	9.26	9.354	1.02	141.4
p193	165	78,7,5,7	4.952	5.017	5.034	0.34	140.2	1.3	9.098	9.232	1.47	140.3
p197	173	99,6,5,7	5.767	5.782	5.794	0.21	160.4	0.25	10.263	10.321	0.57	160.9
p201	177	73,6,4,8	6.053	6.081	6.095	0.23	160.4	0.46	10.945	11.085	1.28	160.5
p216	188	95,7,5,9	5.505	5.529	5.547	0.33	160.5	0.44	10.247	10.294	0.46	160.8
p233	197	88,9,4,10	4.778	5.222	5.258	0.69	160.5	9.27	8.98	9.09	1.22	160
Averages						0.34	119.255	4.20			1.01	122.23

5.3. Surgery fixing and rescheduling

Due to unforeseen reasons, a previously scheduled surgical procedure can be postponed or cancelled. This leads to surgery rescheduling, as highlighted by Burdett and Kozan (2018). It is a challenging but necessary aspect of healthcare management. It requires balancing accommodating patient needs, ensuring patient safety, and efficiently managing resources. While some previously scheduled surgeries can be ultimately rescheduled, often, most of the surgeries closest to execution need to be maintained during the next scheduling. Our approach was developed with initial availability windows for every resource to allow a more flexible input. Some of the reserved initial schedules can also be pre-scheduled surgeries.

As an example of how input can be used for rescheduling efforts, we selected the best-known solution to instance p70, shown in Figure 8, the non-available moments are marked with the colour purple (171, 99, 250), on a 0-255 (red, green, blue) scale. We highlight the schedule of a patient as an example. The patient of colour orange (255, 161, 90) has its events numbered. The patient arrives at the hospital and first goes to Room 12022 - 0 (1), goes to surgery in Room 46048 - 1 (2), leaves to observation in Room 89947 - 3 (3) and moves to recovery back in Room 12022 - 0 (4).

Out of the initial 58 surgeries to be scheduled, we randomly removed 11 to simulate cancelled surgeries, followed by the fixation of programmed schedules of 10 other ones, fixing the rooms, surgeons, and types of equipment reserved for these time intervals. We selected mainly from the first to be performed for the initial scheduling. Finally, we created 7 new surgeries. The

BRKGA-QL was run with the new instance under the same conditions as when p70 was initially solved with ten runs. The room scheduling for the best solution found can be observed in Figure Figure 9. The fixed time intervals are the same colour as the non-business hour intervals for all rooms, marked with red (239, 85, 59). The algorithm could fulfil the ORs' time slots as efficiently as possible without pre-scheduled surgeries.

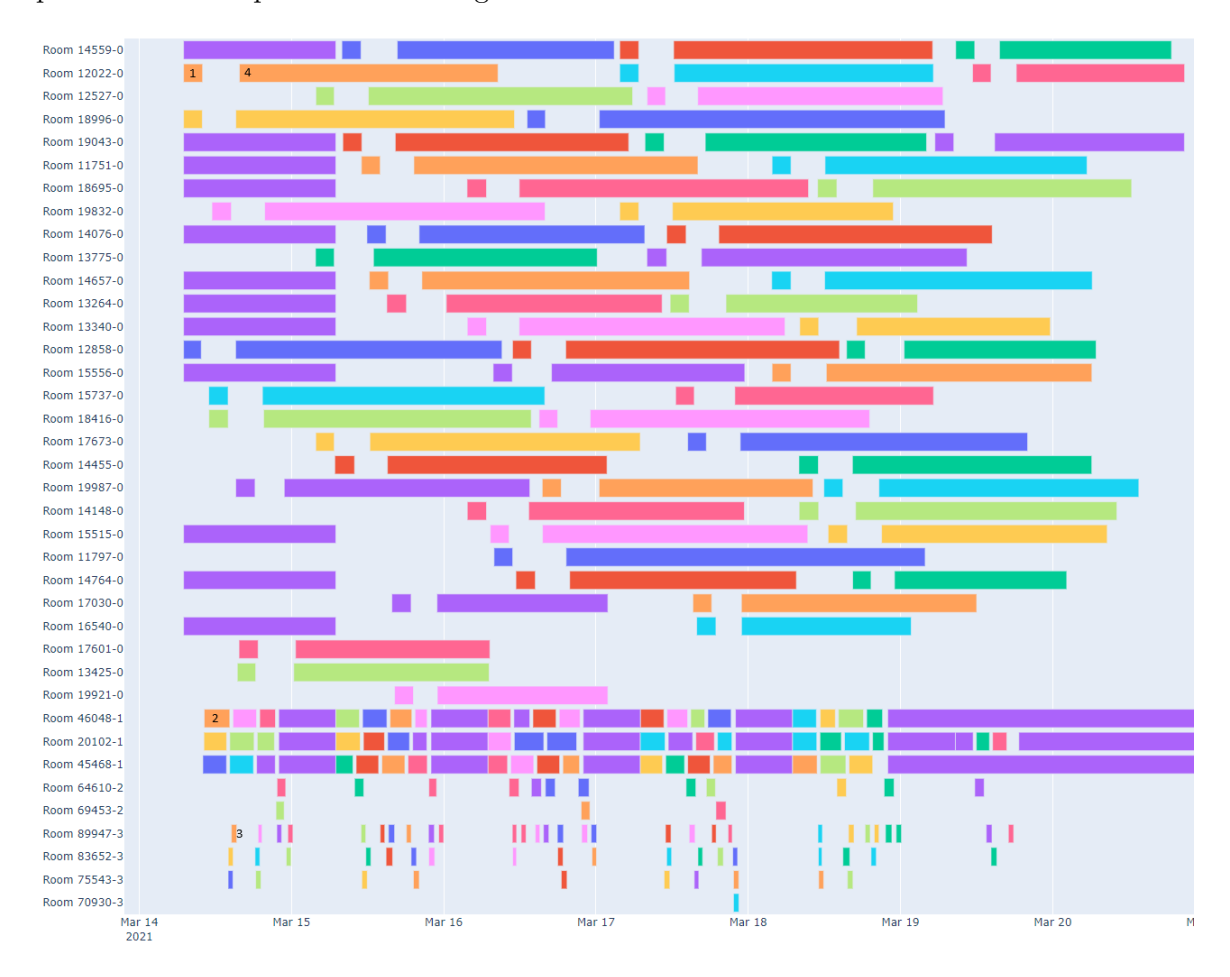


Figure 8: Rooms schedule of the best-known solution to p70.

6. Conclusions and future works

This research highlights the importance of effective surgery scheduling in managing healthcare institutions. The Random Key Optimizer (RKO), incorporating the BRKGA-QL, Simulated Annealing, and Iterated Local Search methods, marks a significant advancement in tackling the complex challenges of surgery scheduling. By carefully managing the availability of rooms, patients, and surgeons, our methods generate efficient schedules and support flexible re-scheduling, aligning with the dynamic demands of healthcare environments.

Using real-world data to generate and test new instances enhances the applicability and relevance of our approach. The introduction of simple lower-bound formulations serves as a critical contribution, enabling a nuanced evaluation of optimality gaps and providing a benchmark for assessing the effectiveness of the heuristic results. Considering the three metaheuristics, the statistical analysis highlights the RKO as a valuable tool for optimizing surgery scheduling in this case study. In this context, BRKGA-QL consistently demonstrates its potential to identify superior solutions, mainly when business hours are considered.

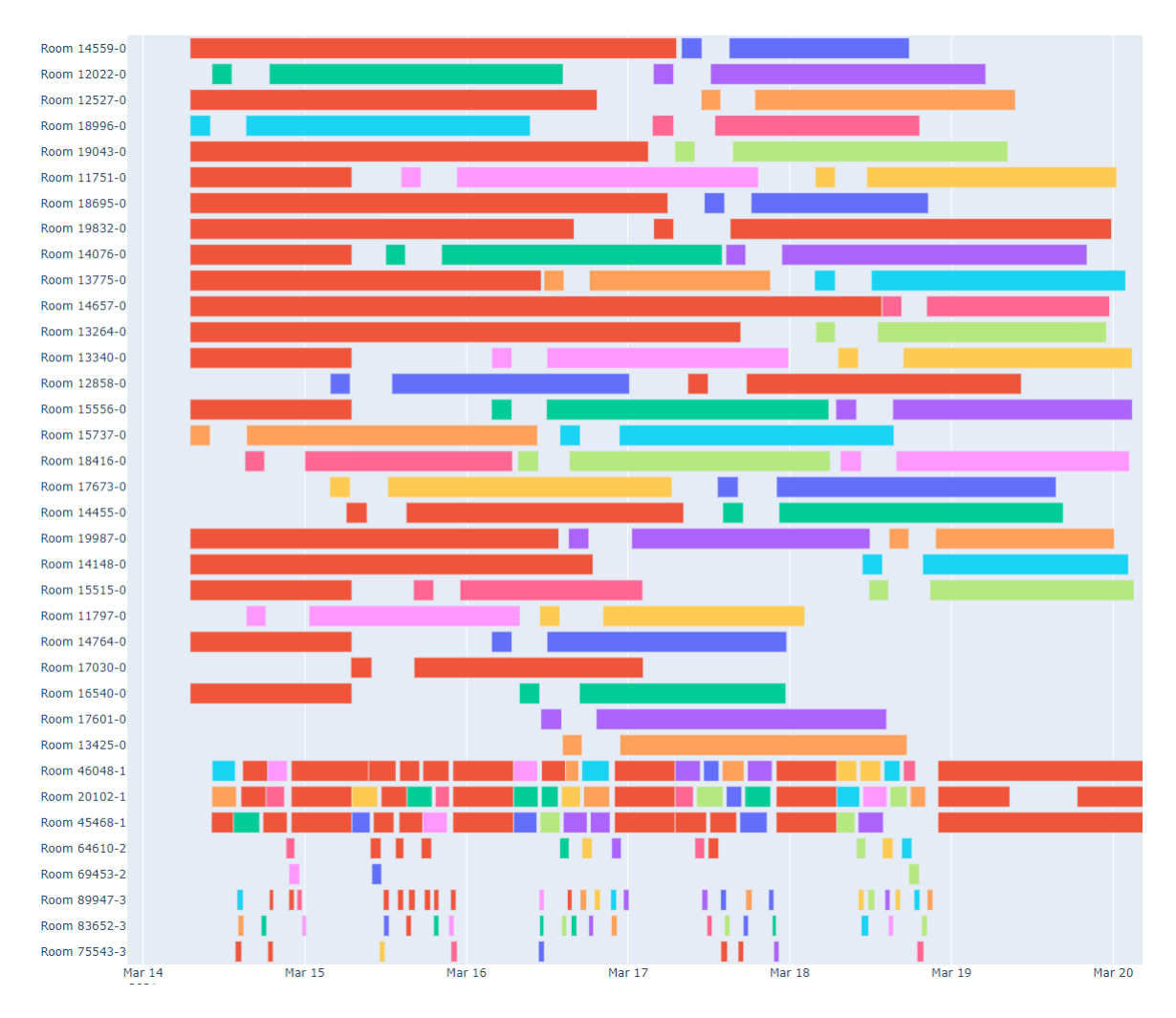


Figure 9: Rooms schedule of a rescheduled solution to p70.

Our research showcases tangible improvements over existing literature instances, demonstrating superior performance across lower and upper bounds. Additionally, the efficiency in generating schedules for the newly introduced instances signifies our method's practical applicability and scalability.

This study contributes substantively to the ongoing discourse on optimizing surgery scheduling, offering practical solutions to healthcare practitioners and administrators. The insights gained from our research can empower hospitals to refine resource allocation, minimize patient wait times, and elevate overall operational efficiency. The proposed RKO approach and its associated formulations stand poised to make enduring contributions to the evolving landscape of healthcare scheduling and optimization.

For future works, we plan to investigate a complete mathematical model for the IORSP and a hybrid exact algorithm that could improve the solution quality and the bounds.

Acknowledgments

This work was supported by the São Paulo Research Foundation (FAPESP) under grant #2021/09482-

- 4. Antonio A. Chaves was supported by FAPESP under grants #2018/15417-8 and #2022/05803-
- 3, and National Council for Scientific and Technological Development (CNPq) under grants

#423694/2018-9 and #303736/2018-6. Eduardo M. Silva was supported by the São Paulo Research Foundation (FAPESP) under grant #2023/04588-4.

References

- Zakaria Abdelrasol, Nermine Harraz, and Amr Eltawil. Operating room scheduling problems: A survey and a proposed solution framework. In Haeng Kon Kim, Sio-Iong Ao, and Mahyar A. Amouzegar, editors, *Transactions on Engineering Technologies*, pages 717–731, Dordrecht, 2014. Springer Netherlands. ISBN 978-94-017-9115-1.
- Rodrigo M Aiex, Mauricio GC Resende, and Celso CR Ribeiro. Ttt plots: a perl program to create time-to-target plots. *Optimization Letters*, 1(4):355–366, 2007.
- Babak Akbarzadeh, Ghasem Moslehi, Mohammad Reisi-Nafchi, and Broos Maenhout. A diving heuristic for planning and scheduling surgical cases in the operating room department with nurse re-rostering. *Journal of Scheduling*, 23(2):265–288, Apr 2020. ISSN 1099-1425. doi: 10.1007/s10951-020-00639-6. URL https://doi.org/10.1007/s10951-020-00639-6.
- Carlos E. Andrade, Thuener Silva, and Luciana S. Pessoa. Minimizing flowtime in a flowshop scheduling problem with a biased random-key genetic algorithm. *Expert Systems with Applications*, 128:67–80, 2019. ISSN 0957-4174. doi: https://doi.org/10.1016/j.eswa.2019.03.007. URL https://www.sciencedirect.com/science/article/pii/S0957417419301605.
- Roberto Aringhieri, Paolo Landa, Patrick Soriano, Elena Tànfani, and Angela Testi. A two level metaheuristic for the operating room scheduling and assignment problem. *Computers & Operations Research*, 54:21–34, 2015. ISSN 0305-0548. doi: https://doi.org/10.1016/j.cor.2014. 08.014. URL https://www.sciencedirect.com/science/article/pii/S030505481400224X.
- J. Baxter. Local optima avoidance in depot location. *Journal of the Operational Research Society*, 32:815–819, 1981.
- James C. Bean. Genetic algorithms and random keys for sequencing and optimization. *ORSA Journal on Computing*, 6(2):154–160, 1994. doi: 10.1287/ijoc.6.2.154. URL https://doi.org/10.1287/ijoc.6.2.154.
- P. Brucker and R. Schlie. Job-shop scheduling with multi-purpose machines. *Computing*, 45(4): 369–375, Dec 1990. ISSN 1436-5057. doi: 10.1007/BF02238804. URL https://doi.org/10.1007/BF02238804.
- Robert L. Burdett and Erhan Kozan. An integrated approach for scheduling health care activities in a hospital. *European Journal of Operational Research*, 264(2):756-773, 2018. ISSN 0377-2217. doi: https://doi.org/10.1016/j.ejor.2017.06.051. URL https://www.sciencedirect.com/science/article/pii/S0377221717305921.
- Imran Ali Chaudhry and Abid Ali Khan. A research survey: review of flexible job shop scheduling techniques. *International Transactions in Operational Research*, 23(3):551–591, 2016. doi: https://doi.org/10.1111/itor.12199. URL https://onlinelibrary.wiley.com/doi/abs/10.1111/itor.12199.
- Antonio A. Chaves, Mauricio G. C. Resende, and Ricardo M. A. Silva. A random-key grasp for combinatorial optimization, 2024. URL https://arxiv.org/abs/2405.18681.
- Antônio Augusto Chaves and Luiz Henrique Nogueira Lorena. An adaptive and near parameter-free brkga using q-learning method. In 2021 IEEE Congress on Evolutionary Computation (CEC), pages 2331–2338, 2021. doi: 10.1109/CEC45853.2021.9504766.

- Altair da Silva Costa. Assessment of operative times of multiple surgical specialties in a public university hospital. *Einstein (Sao Paulo)*, 15:200–205, 2017. doi: 10.1590/S1679-45082017GS3902.
- Nguyen Dang, Leslie Pérez Cáceres, Patrick De Causmaecker, and Thomas Stützle. Configuring irace using surrogate configuration benchmarks. In *GECCO '17: Proceedings of the Genetic and Evolutionary Computation Conference*, GECCO '17, page 243–250, New York, NY, USA, 2017. Association for Computing Machinery. ISBN 9781450349208. doi: 10.1145/3071178.3071238. URL https://doi.org/10.1145/3071178.3071238.
- Lawrence D. Davis, editor. *Handbook of Genetic Algorithms*. Van Nostrand Reinhold, New York, 1991.
- A. Dekkers and E. Aarts. Global optimization and simulated annealing. *Mathematical Programming*, 50(3):367–393, 1991.
- Nico Dellaert and Jully Jeunet. A variable neighborhood search algorithm for the surgery tactical planning problem. *Computers & Operations Research*, 84:216–225, 2017. ISSN 0305-0548. doi: https://doi.org/10.1016/j.cor.2016.05.013. URL https://www.sciencedirect.com/science/article/pii/S0305054816301204.
- Franklin Dexter, Alex Macario, and Rodney D. Traub. Which Algorithm for Scheduling Add-on Elective Cases Maximizes Operating Room Utilization: Use of Bin Packing Algorithms and Fuzzy Constraints in Operating Room Management. *Anesthesiology*, 91(5):1491–1491, 11 1999. ISSN 0003-3022. doi: 10.1097/00000542-199911000-00043. URL https://doi.org/10.1097/00000542-199911000-00043.
- E. D. Dolan and J. J. Moré. Benchmarking optimization software with performance profiles. *Mathematical Programming*, 91(2):201 213, 2002.
- Guillermo Durán, Pablo A. Rey, and Patricio Wolff. Solving the operating room scheduling problem with prioritized lists of patients. *Annals of Operations Research*, 258(2):395–414, Nov 2017. ISSN 1572-9338. doi: 10.1007/s10479-016-2172-x. URL https://doi.org/10.1007/s10479-016-2172-x.
- H. Fei, C. Chu, and N. Meskens. Solving a tactical operating room planning problem by a column-generation-based heuristic procedure with four criteria. *Annals of Operations Research*, 166(1): 91–108, Feb 2009. ISSN 1572-9338. doi: 10.1007/s10479-008-0413-3. URL https://doi.org/10.1007/s10479-008-0413-3.
- H. Fei, N. Meskens, and C. Chu. A planning and scheduling problem for an operating theatre using an open scheduling strategy. *Computers & Industrial Engineering*, 58(2):221–230, 2010. ISSN 0360-8352. doi: https://doi.org/10.1016/j.cie.2009.02.012. URL https://www.sciencedirect.com/science/article/pii/S0360835209000801. Scheduling in Healthcare and Industrial Systems.
- J. F. Gonçalves and M. G. C. Resende. Biased random-key genetic algorithms for combinatorial optimization. *Journal of Heuristics*, 17(5):487–525, 2011.
- Gurobi Optimization, LLC. Gurobi Optimizer Reference Manual, 2023. URL https://www.gurobi.com.
- Mahdi Hamid, Mohammad Mahdi Nasiri, Frank Werner, Farrokh Sheikhahmadi, and Mohammad Zhalechian. Operating room scheduling by considering the decision-making styles of surgical team members: A comprehensive approach. *Computers & Operations Research*, 108:166–181, 2019. ISSN 0305-0548. doi: https://doi.org/10.1016/j.cor.2019.04.010. URL https://www.sciencedirect.com/science/article/pii/S0305054819300930.

- Giorgos Karafotias, Mark Hoogendoorn, and A. E. Eiben. Evaluating reward definitions for parameter control. In Antonio M. Mora and Giovanni Squillero, editors, *Applications of Evolutionary Computation*, pages 667–680, Cham, 2015. Springer International Publishing. ISBN 978-3-319-16549-3.
- S. Kirkpatrick, C. D. Gelatt, and M. P. Vecchi. Optimization by simulated annealing. *Science*, 220(4598):671–680, 1983.
- Paolo Landa, Roberto Aringhieri, Patrick Soriano, Elena Tànfani, and Angela Testi. A hybrid optimization algorithm for surgeries scheduling. *Operations Research for Health Care*, 8:103–114, 2016. ISSN 2211-6923. doi: https://doi.org/10.1016/j.orhc.2016.01.001. URL https://www.sciencedirect.com/science/article/pii/S2211692315300084.
- Yang-Kuei Lin and Min-Yang Li. Solving operating room scheduling problem using artificial bee colony algorithm. *Healthcare*, 9(2), 2021. ISSN 2227-9032. doi: 10.3390/healthcare9020152. URL https://www.mdpi.com/2227-9032/9/2/152.
- Ya Liu, Chengbin Chu, and Kanliang Wang. A new heuristic algorithm for the operating room scheduling problem. Computers & Industrial Engineering, 61(3):865-871, 2011. ISSN 0360-8352. doi: https://doi.org/10.1016/j.cie.2011.05.020. URL https://www.sciencedirect.com/science/article/pii/S0360835211001458.
- H. R. Lourenço, O. Martin, and T. Stützle. Iterated local search. In *Handbook of Metaheuristics*, International Series in Operations Research & Management Science, pages 321–353. Kluwer Academic Publishers, 2003. ISBN 978-1-4020-7263-5.
- A. D. Mangussi, H. Pola, H. G. Macedo, L. A. Juli ao, M. P. T. Proença, P. R. L. Gianfelice, B. V. Salezze, and A. A. Chaves. Meta-heurísticas via chaves aleatórias aplicadas ao problema de localização de hubs em árvore. In *Anais do Simpósio Brasileiro de Pesquisa Operacional*, São José dos Campos, 2023. Galoá.
- Inês Marques and M. Eugénia Captivo. Bicriteria elective surgery scheduling using an evolutionary algorithm. Operations Research for Health Care, 7:14-26, 2015. ISSN 2211-6923. doi: https://doi.org/10.1016/j.orhc.2015.07.004. URL https://www.sciencedirect.com/science/article/pii/S2211692314200580. ORAHS 2014 The 40th international conference of the EURO working group on Operational Research Applied to Health Services.
- Nicholas Metropolis, Arianna Rosenbluth, Marshall Rosenbluth, Augusta Teller, and Edward Teller. Equation of state calculations by fast computing machines. *Journal of Chemical Physics*, 21:1087–1092, 1953.
- N. Mladenović and P. Hansen. Variable neighborhood search. Computers & Operations Research, 24(11):1097–1100, 1997. ISSN 0305-0548. doi: https://doi.org/10.1016/S0305-0548(97)00031-2. URL https://www.sciencedirect.com/science/article/pii/S0305054897000312.
- Jose M. Molina-Pariente, Victor Fernandez-Viagas, and Jose M. Framinan. Integrated operating room planning and scheduling problem with assistant surgeon dependent surgery durations. Computers & Industrial Engineering, 82:8-20, 2015. ISSN 0360-8352. doi: https://doi.org/10.1016/j.cie.2015.01.006. URL https://www.sciencedirect.com/science/article/pii/S0360835215000157.
- J. A. Nelder and R. Mead. A simplex method for function minimization. *The Computer Journal*, 7(4):308–313, 1965.

- I. Niven, H. S. Zuckerman, and H. L. Montgomery. An Introduction to the Theory of Numbers. John Wiley & Sons, 1991.
- Irem Ozkarahan. Allocation of surgical procedures to operating rooms. *Journal of Medical Systems*, 19(4):333–352, Aug 1995. ISSN 1573-689X. doi: 10.1007/BF02257264. URL https://doi.org/10.1007/BF02257264.
- Jaesang Park, Byung-In Kim, Myungeun Eom, and Byung Kwan Choi. Operating room scheduling considering surgeons' preferences and cooperative operations. *Computers & Industrial Engineering*, 157:107306, 2021. ISSN 0360-8352. doi: https://doi.org/10.1016/j.cie.2021.107306. URL https://www.sciencedirect.com/science/article/pii/S0360835221002102.
- P. H. V. Penna, A. Subramanian, and L. S. Ochi. An iterated local search heuristic for the heterogeneous fleet vehicle routing problem. *Journal of Heuristics*, 19:201–232, 2013.
- Iman Rahimi and Amir H. Gandomi. A comprehensive review and analysis of operating room and surgery scheduling. Archives of Computational Methods in Engineering, 28(3):1667–1688, May 2021. ISSN 1886-1784. doi: 10.1007/s11831-020-09432-2. URL https://doi.org/10.1007/s11831-020-09432-2.
- Vahid Roshanaei, Curtiss Luong, Dionne M. Aleman, and David R. Urbach. Collaborative operating room planning and scheduling. *INFORMS Journal on Computing*, 29(3):558–580, 2017. doi: 10.1287/ijoc.2017.0745. URL https://doi.org/10.1287/ijoc.2017.0745.
- Vahid Roshanaei, Kyle E.C. Booth, Dionne M. Aleman, David R. Urbach, and J. Christopher Beck. Branch-and-check methods for multi-level operating room planning and scheduling. *International Journal of Production Economics*, 220:107433, 2020. ISSN 0925-5273. doi: https://doi.org/10.1016/j.ijpe.2019.07.006. URL https://www.sciencedirect.com/science/article/pii/S0925527319302439.
- Martin J.A. Schuetz, J. Kyle Brubaker, Henry Montagu, Yannick van Dijk, Johannes Klepsch, Philipp Ross, Andre Luckow, Mauricio G.C. Resende, and Helmut G. Katzgraber. Optimization of robot-trajectory planning with nature-inspired and hybrid quantum algorithms. *Phys. Rev. Appl.*, 18:054045, Nov 2022. doi: 10.1103/PhysRevApplied.18.054045. URL https://link.aps.org/doi/10.1103/PhysRevApplied.18.054045.
- Cecília L. Siqueira, Edilson F. Arruda, Laura Bahiense, Germana L. Bahr, and Geraldo R. Motta. Long-term integrated surgery room optimization and recovery ward planning, with a case study in the brazilian national institute of traumatology and orthopedics (into). European Journal of Operational Research, 264(3):870–883, 2018a. ISSN 0377-2217. doi: https://doi.org/10.1016/j.ejor.2016.09.021. URL https://www.sciencedirect.com/science/article/pii/S0377221716307573.
- Cecília L. Siqueira, Edilson F. Arruda, Laura Bahiense, Germana L. Bahr, and Geraldo R. Motta. Long-term integrated surgery room optimization and recovery ward planning, with a case study in the brazilian national institute of traumatology and orthopedics (into). European Journal of Operational Research, 264(3):870–883, 2018b. ISSN 0377-2217. doi: https://doi.org/10.1016/j.ejor.2016.09.021. URL https://www.sciencedirect.com/science/article/pii/S0377221716307573.
- William Spears and Kenneth De Jong. On the virtues of parametrized uniform crossover. In *ICGA*, pages 230–236, 01 1991.

- Richard S. Sutton and Andrew Barto. Reinforcement Learning. *Journal of Cognitive Neuroscience*, 11(1):126–134, 01 1999. ISSN 0898-929X. doi: 10.1162/089892999563184. URL https://doi.org/10.1162/089892999563184.
- A.J. Thomas Schneider, J. Theresia van Essen, Mijke Carlier, and Erwin W. Hans. Scheduling surgery groups considering multiple downstream resources. *European Journal of Operational Research*, 282(2):741–752, 2020. ISSN 0377-2217. doi: https://doi.org/10.1016/j.ejor.2019.09. 029. URL https://www.sciencedirect.com/science/article/pii/S0377221719307854.
- Masoumeh Vali, Khodakaram Salimifard, Amir H. Gandomi, and Thierry J. Chaussalet. Application of job shop scheduling approach in green patient flow optimization using a hybrid swarm intelligence. *Computers & Industrial Engineering*, 172:108603, 2022. ISSN 0360-8352. doi: https://doi.org/10.1016/j.cie.2022.108603. URL https://www.sciencedirect.com/science/article/pii/S0360835222005988.
- J. Theresia van Essen, Joël M. Bosch, Erwin W. Hans, Mark van Houdenhoven, and Johann L. Hurink. Reducing the number of required beds by rearranging the or-schedule. *OR Spectrum*, 36(3):585–605, Jul 2014. ISSN 1436-6304. doi: 10.1007/s00291-013-0323-x. URL https://doi.org/10.1007/s00291-013-0323-x.
- Carla Van Riet and Erik Demeulemeester. Trade-offs in operating room planning for electives and emergencies: A review. *Operations Research for Health Care*, 7:52–69, 2015. ISSN 2211-6923. doi: https://doi.org/10.1016/j.orhc.2015.05.005. URL https://www.sciencedirect.com/science/article/pii/S2211692314200646. ORAHS 2014 The 40th international conference of the EURO working group on Operational Research Applied to Health Services.
- V. Černý. Thermodynamical approach to the traveling salesman problem: An efficient simulation algorithm. *Journal of Optimization Theory and Applications*, 45(1):41–51, 1985.
- Christopher J. C. H. Watkins and Peter Dayan. Q-learning. *Machine Learning*, 8(3):279–292, May 1992. ISSN 1573-0565. doi: 10.1007/BF00992698. URL https://doi.org/10.1007/BF00992698.
- Wei Xiang, Jiao Yin, and Gino Lim. An ant colony optimization approach for solving an operating room surgery scheduling problem. *Computers & Industrial Engineering*, 85:335–345, 2015. ISSN 0360-8352. doi: https://doi.org/10.1016/j.cie.2015.04.010. URL https://www.sciencedirect.com/science/article/pii/S036083521500159X.
- M. Yazdi, M. Zandieh, and H. Haleh. A mathematical model for scheduling elective surgeries for minimizing the waiting times in emergency surgeries. *International Journal of Engineering*, 33 (3):448–458, 2020. ISSN 1025-2495. doi: 10.5829/ije.2020.33.03c.09. URL https://www.ije.ir/article_104670.html.
- Shuwan Zhu, Wenjuan Fan, Tongzhu Liu, Shanlin Yang, and Panos M. Pardalos. Dynamic three-stage operating room scheduling considering patient waiting time and surgical overtime costs. *Journal of Combinatorial Optimization*, 39(1):185–215, Jan 2020. ISSN 1573-2886. doi: 10.1007/s10878-019-00463-5. URL https://doi.org/10.1007/s10878-019-00463-5.

Appendix A. Model bounded by Beds

Formulation (A.1)-(A.5) assumes that beds are the scheduling bottleneck. Our only decision variable x_{rk} is a binary one that indicates whether surgery k is allocated to bed r ($x_{rk} = 1$) or not ($x_{rk} = 0$).

The objective function (A.1) minimizes the best case makespan, Constraints (A.2) calculate the minimal allocated time for each room, where $T_k^T := \sum_{t \in T_k} \gamma_t^d + \gamma_t^m$ is the minimal total time the patient from surgery s takes from arriving at the hospital until discharge (sum of duration γ_t^d and moving γ_t^m times), Constraints (A.3) ensure each surgery is allocated to some room. Constraint (A.4) allocates an arbitrary surgery to a room for symmetry breaking, we display the surgery 0 being allocated to bed 0, and Constraints (A.5) state all x_{rk} variables as binary.

$$Minimize \ z_1$$
 (A.1)

Subject to:

$$\sum_{k \in K} T_k^T x_{rk} \le z_1 \tag{A.2}$$

$$\sum_{r \in R^{bed}} x_{rk} = 1 \tag{A.3}$$

$$x_{00} = 1 \tag{A.4}$$

$$x_{rk} \in \{0,1\}$$
 $\forall r \in R^{bed} \quad \forall k \in K \text{ (A.5)}$

Appendix B. Model bounded by Operation Rooms

The other proposed solution, Formulation (B.1)-(B.7), also offers a relaxed approach to solving the IORSP. It assumes that ORs are the scheduling bottleneck. Our objective function, (B.1), minimizes the hypothetical makespan. Constraints (B.2) estimate the best possible makespan for each OR, where $T_k^F := \gamma_{First(k)}^d + \gamma_{First(k)}^m$ is the duration and moving times before the OR for surgery k, T_k^S is the surgery added to the moving time after it and T_k^L is the sum of all duration and transfer times after the OR task. Analogous to these constants, we have our binary decision variables, f_{rk} indicating if surgery k is the first one allocated to OR r, x_{rk} indicates if surgery k is allocated to OR r and l_{rk} indicates if surgery k is the last one allocated to OR r.

Constraints (B.3) ensure that all surgeries are allocated to a room, while Constraints (B.4) and (B.5) ensure that each OR has a first and last scheduled surgery. Constraints (B.6) ensure that surgery k can only be the first or last if it is allocated to the respective OR, while Constraints (B.7) define all x_{rk} , f_{rk} , and l_{rk} variables as binary.

$$Minimize z_2$$
 (B.1)

Subject to:

$$\sum_{k \in K_r} (T_k^F f_{rk} + T_k^S x_{rk} + T_k^L l_{rk}) \le z_2 \qquad \forall r \in \mathbb{R}^{or}$$
(B.2)

$$\sum_{r \in R^{or}} x_{rk} = 1 \qquad \forall k \in K$$
 (B.3)

$$\sum_{k \in K_r} f_{rk} = 1 \qquad \forall \ r \in R^{or} \tag{B.4}$$

$$\sum_{k \in K_r} l_{rk} = 1 \qquad \forall r \in R^{or} \tag{B.5}$$

$$x_{rk} \ge f_{rk} + l_{rk}$$
 $\forall r \in R^{or} \quad \forall k \in K_r$ (B.6)

$$x_{rk}, f_{rk}, l_{rk} \in \{0, 1\}$$

$$\forall r \in \mathbb{R}^{or} \quad \forall k \in K_r \text{ (B.7)}$$

Appendix C. Lower bound computations

Table C.9 shows the results of our proposed models with the literature instances. For each instance is shown its name, number of surgeries, and number of rooms sorted by room type (for instance "CASE_10", using our nomenclature, there are 5 beds, 4 ORs, 5 ICUs, and 20 wards) and the computed lower bound and CPU time spent for each model.

Analysing the results, the model bounded by ORs (B.1-B.7) is much easier to solve than that bounded by Beds (A.1-A.5). In contrast, only seven out of the 24 instances have optimal lower bounds with 3600 seconds, while all computed lower bounds by the OR model are optimal. Our statistical testing showed the Model Bed to generate superior bounds with p-value = 0.0000035. Thus, the instances are more bounded by Bed availability by a large margin.

Table C.9: Literature instances formulation results.

Model			Bed		OR	
Instance	Surgeries	Rooms	Lower Bound	Time(s)	Lower Bound	Time(s)
CASE_01	50	5,2,5,10	16.41	3600.01	4.57	0.01
$CASE_02$	100	5,2,5,10	35.32	340.21	7.89	0.01
$CASE_03$	150	5,2,5,10	49.06	243.07	11.69	0.01
CASE_04	200	5,2,5,10	67.05	355.09	14.93	0.01
$CASE_05$	50	5,3,5,10	16.88	3600.01	3.72	0.02
CASE_06	100	5,3,5,10	32.94	145.64	5.97	0.02
$CASE_07$	150	5,3,5,10	48.81	95.60	7.89	0.03
CASE_08	200	5,3,5,10	67.50	281.53	10.09	0.02
$CASE_{-}09$	50	5,4,5,20	7.60	3600.01	2.85	0.10
CASE_10	100	5,4,5,20	16.53	3600.02	4.64	0.02
$CASE_11$	150	5,4,5,20	24.31	3600.01	5.92	0.06
$CASE_{-12}$	200	5,4,5,20	33.60	3600.02	7.73	0.04
$CASE_13$	50	5,5,5,20	8.11	3600.01	2.67	0.19
CASE_14	100	5,5,5,20	16.92	3600.01	3.91	0.07
$CASE_15$	150	5,5,5,20	25.50	3600.01	5.10	0.10
CASE_16	200	5,5,5,20	35.27	3600.01	6.66	0.04
$CASE_17$	50	5,10,5,20	9.03	3600.01	2.44	65.02
CASE_18	100	$5,\!10,\!5,\!20$	16.99	3600.01	2.70	50.53
$CASE_19$	150	5,10,5,20	26.23	3600.01	3.29	0.64
$CASE_20$	200	$5,\!10,\!5,\!20$	33.55	3600.01	3.96	19.58
$CASE_21$	50	5,10,5,30	6.09	0.51	2.36	76.05
$CASE_22$	100	5,10,5,30	11.05	3600.16	2.62	15.84
$CASE_23$	150	$5,\!10,\!5,\!30$	15.70	3600.02	3.27	160.01
$CASE_24$	200	5,10,5,30	21.26	3600.01	3.90	95.01
Average ti	mes			3450.01		43.04
Averages 1	RPD(%)		0.000		77.321	

We can visualise this attribute in Figure C.10, a heuristic solution of "CASE_01". Each unique colour represents a patient, and we can observe that all rooms, except for beds, have sparse allocations. A bed is reserved from the moment the patient enters a Ward. This explains the empty spaces between the bed usages; however, they are fully utilized.

Table C.10 shows the results of our proposed models with the case study instances. For each instance, the instances' names, number of surgeries, number of rooms sorted by room type, the computed lower bound in days, and CPU time spent for each model type are presented. Analyzing the results, we can observe that 16 instances were more bounded by OR availability and four by Bed availability. The statistical testing shows that the OR formulation computed better bounds with p-value = 0.005162. This shows some balance during the instances' procedural generation. As in the literature instances, the model bounded by ORs is much easier to solve than the model bounded by Beds, whereas only nine out of the 20 instances have optimal lower bounds within 3600 seconds, and all computed lower bounds by the OR model are optimal.

To visualize how a solution with all the availability slots looks like, Figure C.11 shows the Gantt view of the best solution of instance p098 without availability slots. We can observe that the operating rooms are allocated very close to the limit of their capacity, and the last occupied beds are released almost simultaneously, not as well distributed as in Figure C.10.

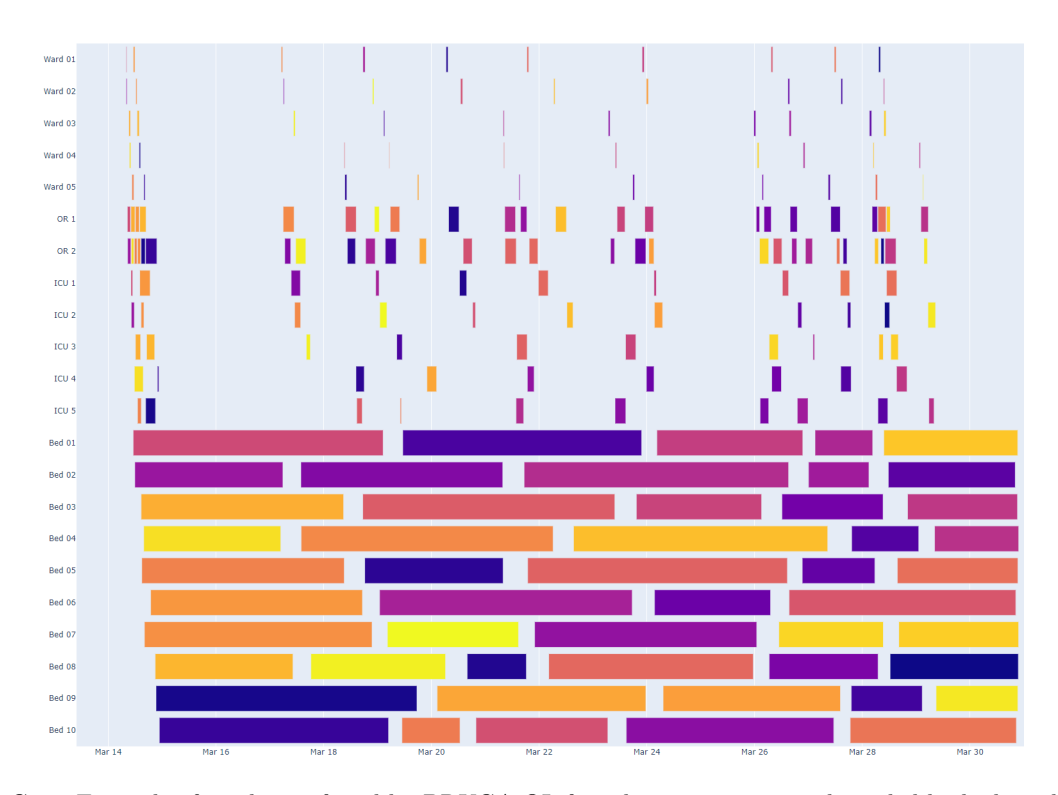


Figure C.10: Example of a solution found by BRKGA-QL for a literature instance bounded by bed availability.

Table C.10: Case study instances formulation results. $\mid \quad \text{Bed} \quad \mid \quad \text{OR}$

Model			Bed		OR	
Instance	Surgeries	Rooms	Lower Bound	Time(s)	Lower Bound	Time(s)
p070	58	31,3,2,4	3.899	0.32	4.440	0.01
p078	66	23,3,3,4	5.536	3600.02	4.722	0.07
p087	75	29,3,3,4	5.247	3600.02	5.146	0.06
p093	81	30,3,3,4	5.253	3600.01	5.485	0.07
p098	86	40,3,2,4	4.444	26.32	5.719	0.02
p100	84	39,4,3,5	4.486	3600.03	4.604	0.14
p109	93	35,4,3,5	5.364	3600.01	5.015	0.36
p120	104	46,4,4,5	4.699	3600.03	5.466	0.46
p138	118	43,5,4,5	5.224	3600.01	4.945	0.04
p153	133	71,5,4,7	3.823	2.32	5.486	0.09
p165	141	78,6,4,7	3.895	4.76	5.019	5.69
p178	154	88,6,4,6	3.848	2.89	5.335	1.09
p183	159	89,6,4,6	3.875	282.51	5.556	1.76
p189	161	71,7,5,7	4.849	2912.48	4.902	8.45
p192	164	72,7,4,8	4.701	3600.01	4.964	3.97
p193	165	78,7,5,7	4.113	3600.02	4.952	13.92
p197	173	99,6,5,7	3.829	30.11	5.767	3.16
p201	177	73,6,4,8	4.875	3600.03	6.053	5.82
p216	188	95,7,5,9	3.842	24.05	5.505	3.19
p233	197	88,9,4,10	4.484	3600.08	4.778	36.02
Averages				2144.302		4.220
Averages	RDP(%)		13.944		1.424	

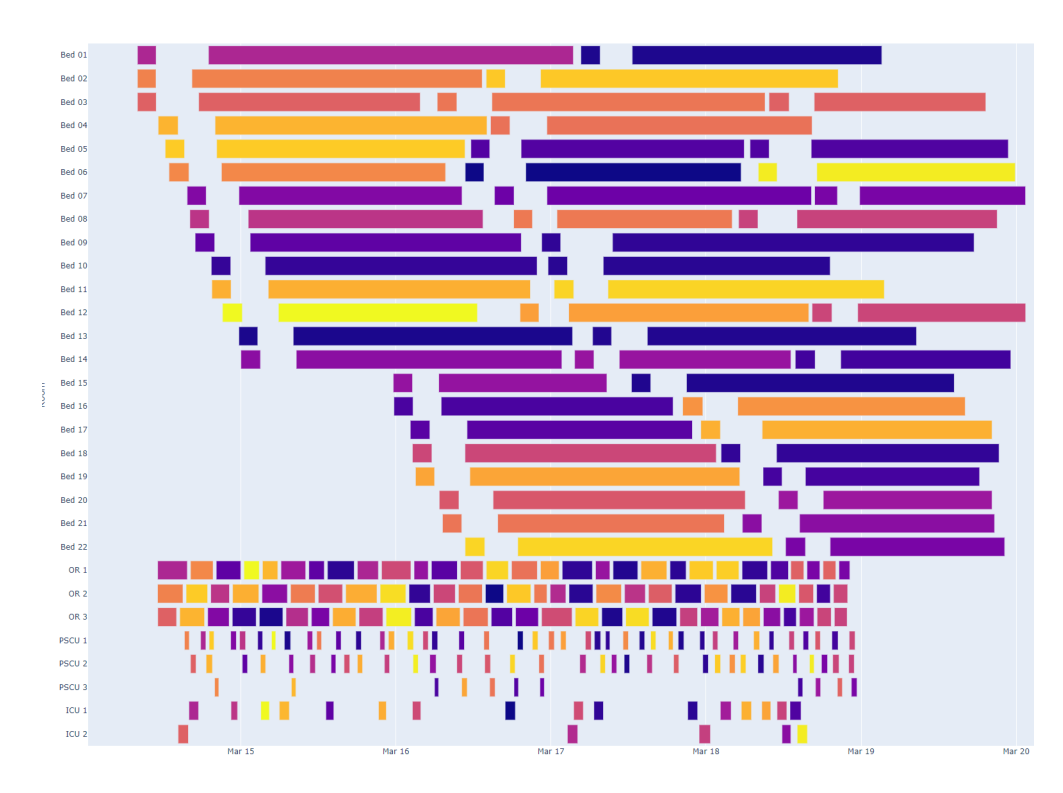


Figure C.11: Example of a solution found by BRKGA-QL for a case study instance bounded by OR availability.